FCP Report No. 14

EFFECTS OF GRAPHITE MORPHOLOGY, MATRIX HARDNESS AND STRUCTURE ON THE FATIGUE RESISTANCE OF GRAY CAST IRON

by

M. R. Mitchell
Department of Theoretical and Applied Mechanics

ABSTRACT

The fatigue resistance of gray cast iron is shown to be strongly dependent on graphite morphology and the strength of the steel-like matrix. Considering graphite flakes in gray iron as "internal notches," a comparison is made of the fatigue resistance of gray irons and steels of comparable composition, hardness, and microstructure. Application of a Neuber analysis, previously employed in geometrically notched members to relate nominal stresses and strains to local stresses and strains at notch roots, produces quantitative values of the fatigue notch factor, K_f, for various graphite morphologies, matrix structures and hardnesses. Fatigue resistance of gray irons is enhanced by decreasing graphite flake size. Matrix hardness is of greater importance than structure in determining the fatigue resistance.

A Report of the
FRACTURE CONTROL PROGRAM

College of Engineering, University of Illinois
Urbana, Illinois 61801
December, 1974

ACKNOWLEDGMENTS

Research presented here was sponsored by and conducted at Ford Motor Company, Scientific Research Staff, Detroit, Michigan, and is a portion of a three-year corporate investigation on the fatigue behavior of gray iron (1968-70). The author is grateful to Drs. T. L. Johnston and C. E. Feltner, then Managers of the Metallurgy Department, for their interest in this project and Dr. N. A. Gjostein, presently Manager of the Metallurgy Department, for permission to openly publish these findings as a Fracture Control Program report. The manuscript has been submitted to SAE for presentation at the annual meeting in Detroit, Michigan, February 24-28, 1975.

Technical discussions, criticisms, and manuscript reviews of Dr. R. W. Landgraf, Ford Motor Company, and Professor JoDean Morrow, University of Illinois, were helpful and are graciously acknowledged. Mrs. Darlene Mathine patiently typed the manuscript, and Mr. Arthur Mak prepared the figures for this report.

INTRODUCTION

Employing monotonic and cyclic stress-strain properties to qualitatively predict the fatigue resistance of wrought metals has become generally accepted (1). However, using such properties as an indication of the fatigue resistance of cast metals can result in serious error (2), since cast metals are microflawed structures.

Viewing gray cast iron as internally notched steel, Neuber's notch analysis is employed and comparison made of the fatigue resistance of steels matched in hardness, composition and structure to the matrices of several gray irons. Quantitative values of the fatigue notch factors (K_f) associated with various graphite morphologies and matrix structures are presented.

CAST IRONS AND STEELS EMPLOYED FOR THE NOTCH ANALYSIS

Shown in Fig. 1 are the matrix structures and graphite morphologies used in this investigation. In total, ten systems are employed in this investigation:

SAE 9262 Steel:

(A) Pearlitic Matrices (DPH = 272)*

(B) Martensitic Matrices (DPH = 286)

(C) Martensitic Matrices (DPH = 434)

Gray Cast Irons:

(A) Pearlitic Matrices (DPH = 272)**

(1) Coarse Graphite

(2) Fine Graphite

(3) Mixed Graphite

---

*All hardnesses reported are an average of five DPH measurements per sample.

**Hardnesses for the gray cast irons are matrix hardnesses and not "bulk" hardnesses.

Gray Cast Irons (Continued):

(B) Martensitic Matrices (DPH = 434)

(1) Coarse Graphite

(2) Fine Graphite

(3) Mixed Graphite

(C) Martensitic Matrices (DPH = 286) with Mixed Graphite

SPECIMEN PREPARATION

Steel:

A twenty-pound vacuum melt of a steel similar to SAE 9262 was cast under an inert argon atmosphere to prevent oxidation and reduce inclusion formation. Table 1 gives a comparison of the compositions of this steel melt and the cast irons. The steel ingot was hot reduced to approximately 5/8 inch diameter and normalized in an inert atmosphere. Subsequent heat treatments, given in Appendix A, were performed to produce the desired matrix structures and hardness. Specimens of the design, shown in Fig. 2, were machined for mechanical tests.*

Cast Iron:

Arbitration bars were cast by Cleveland Iron Foundry (Ford Motor Company) from the same melt in 4 inch and 7/8 inch diameters. This was done to produce different solidification rates with a resultant difference in graphite morphologies while maintaining (approximately) the same nominal matrix composition. Micrographs of these cast irons are shown in Fig. 3. Both irons have ASTM graphite type "A", but with sizes near the extremes of the ASTM standard chart.** The "fine" structure is

---

*Testing was performed with a $\pm$ 20 kip closed loop, electrohydraulic test system.

**ASTM - A - 247, Plate I

size 5-7 while the "coarse" structure is size 3-4. As-cast matrices of these irons are pearlitic. These irons as well as a specially inoculated iron with "mixed" graphite structure (nominally 60% type A graphite, size 4-5; 40% type D), also shown in Fig. 3, were made into specimens of the design, shown in Fig. 4.

MECHANICAL BEHAVIOR OF SAE 9262 STEEL

Monotonic and Cyclic Stress-Strain Results:

Typical monotonic and cyclic stress-strain curves of SAE 9262 in the pearlitic and two martensitic conditions are shown in Figs. 5, 6 and 7, respectively. It is apparent from these figures that the pearlitic matrix cyclically hardens* while the higher hardness martensite cyclically softens and the lower hardness martensite exhibits mixed behavior (i.e., softens, then hardens). These deformation responses are typical of steels and would be expected in the matrix of a similar cast iron. However, because graphite flakes are present, the bulk response of cast irons is cyclically stable as will be shown later.

Monotonic and cyclic material property data determined from the stress-strain curves for the steels are given in Tables 2, 3 and 4. Note the true fracture ductilities (ϵ_f) of the steels with the martensitic matrices are similar to each other, but greater than for the pearlite. Thus, the pearlitic steel should have decreased short life fatigue resistance. Long life fatigue resistance of wrought metals, dependent primarily on the true fracture strength, should be superior for the hard martensite because of its superior true fracture strength (σ_f).

---

*The cyclic stress-strain curve is above the monotonic stress-strain curve.

Fatigue Behavior:

Results of axial, constant strain amplitude tests for the steels are given in Table 5 and the strain-life curves are shown in Figs. 8, 9 and 10. Pearlite, having the lower fracture ductility, has an inferior short life fatigue resistance compared to the martensites. Also evident (Fig. 10) is the superior long life fatigue resistance of the harder martensite.

In the following section, monotonic and cyclic stress-strain response and the strain-life fatigue behavior of cast irons with three different graphite morphologies are presented. It should be remembered that the matrix structures of the cast irons are identical in composition, hardness and structure to the SAE 9262 steel discussed above.

MECHANICAL BEHAVIOR OF PEARLITIC AND MARTENSITIC GRAY CAST IRONS

In this section attention will be focused on the monotonic stress-strain response and strain-life behavior of cast irons with varying graphite structures and both pearlitic and martensitic matrices.

Monotonic and Cyclic Stress-Strain Results:

Monotonic tension and compression stress-strain curves are shown in Figs. 11, 12 and 13 for the three pearlitic, as-cast irons. Mechanical properties are given in Tables 6, 7 and 8. The ultimate strengths (S_u) in tension are found to be approximately one-third that in compression. The initial tangent modulii (E) are seen to increase with the finer graphite structures as do the fracture ductilities (ϵ_f). Also, the true toughness (U_p), which is a measure of the energy to cause failure (3), increases with finer graphite structures.

Superimposed on the monotonic stress-strain curve in Fig. 13 is the cyclic stress-strain curve for the mixed graphite, pearlitic cast iron. This cyclic stress-strain curve was obtained from the saturation stress values taken from the tips of stabilized hysteresis loops of constant strain amplitude tests (4) reported in a subsequent section. It should be noted that the monotonic tension and cyclic tension stress-strain curves are essentially the same as are the corresponding compression curves. Thus, the bulk response of this cast iron is cyclically stable, and the monotonic stress-strain curve adequately describes the cyclic response. This does not imply that the response of the matrix of the cast iron is cyclically stable. As shown in Fig. 14, there is an increase in the matrix hardness of the cast iron with increased strain amplitudes. This indicates that the matrix is cyclically hardening locally while the bulk response remains stable.

Monotonic tension and compression curves for the four martensitic cast irons are shown in Figs. 15 through 18. It is apparent from the mechanical properties given in Tables 9 through 12 that there is a definite strength increase obtainable by increasing the hardness through heat treatment. There is, however, an accompanying decrease in ductility which is common for most metals (5). The mixed graphite martensitic iron, tempered to DPH = 286, does not differ significantly in strength or ductility from its pearlitic matrix counterpart (DPH = 272).

Fatigue Behavior:

Several specimens each of the pearlitic and martensitic cast irons with the three graphite morphologies, as well as the low hardness martensite with the mixed graphite structure, were tested under completely reversed, axial, constant strain amplitude control conditions (6). Results of these fatigue tests are given in Tables 13 through 15 and shown in Figs. 19 through 22. The coarser graphite gray iron is seen to be inferior to the finer graphite gray irons. In fact, extrapolating to 10^8 reversals the

coarser graphite iron is a factor of two in strain less fatigue resistant than the mixed graphite gray iron (0.0005 as compared to 0.001). In comparison to the fatigue resistance of the similar steel (see Fig. 8), the introduction of the coarse graphite flakes in an otherwise homogeneous steel matrix (the cast iron) causes a decrease in fatigue resistance of more than a factor of three in strain upon extrapolation to 10^8 reversals (0.0005 as compared to 0.018).

The mixed graphite structure does not cause as great a decrease in strain fatigue resistance when compared to the steel (0.001 as compared to 0.018). Also, there is a very noticeable decrease in the transition fatigue lives* due to the introduction of these internal flaws in the steel matrix. For example, the value of the transition fatigue life for the pearlitic steel is approximately 4×10^3 reversals while that of the mixed graphite cast iron with the pearlitic matrix is approximately 12 reversals (2). This indicates that the fatigue resistance of gray cast iron is dependent primarily on the fracture strength (σ_f). However, as will be shown, the greater ultimate strengths resulting from increasing the matrix hardness by heat treatment is not necessarily beneficial to fatigue resistance.

The strain-life behavior of the high hardness martensitic iron with coarse graphite is essentially the same as its softer pearlitic complement even though the martensite has approximately a 20% greater ultimate strength. As mentioned previously, the greater strength should be conducive to improved long-life fatigue resistance (in wrought materials). Similarity in the behavior of these different hardness irons is felt to be due to the effect of the internal flaws or notches much the same as has been demonstrated with notches in steels (7). "Coarser" notches are less effective in reducing the notch sensitivity, which is a relative measure of notch effectiveness,

---

*The point on a strain-life diagram where the elastic and plastic strain components of total strain are equal.

than the "finer" notches. Progressively finer graphite structures are seen to be more effective with increased matrix hardness when comparison is made of the strain amplitudes at 10^8 reversals in Figs. 19 and 20 as well as 21.

The most drastic reduction in fatigue resistance is with the mixed graphite, high hardness martensite which is approximately 40% less fatigue resistant in strain than its pearlitic complement. Conversely, the mixed graphite, low hardness martensite and its pearlitic complement have approximately the same fatigue resistance. It may be concluded, therefore, that in the hardness ranges investigated the matrix structure is of less importance in controlling the fatigue resistance of cast iron than the graphite size and matrix hardness. The best strain fatigue resistance in this investigation is obtained from fine graphite types and the softer, more compliant, pearlitic matrices.

NEUBER ANALYSIS

In this section, a comparison is made of the steels and matching cast iron structures to determine the quantitative effectiveness of these internal flaws in reducing the fatigue resistance of the cast iron. This is accomplished by employing a Neuber analysis which relates the nominal stress-strain behavior of a notched member to the local stress-strain behavior at the notch root.

Topper, et al. (8) presented a procedure for predicting the fatigue behavior of notched specimens from smooth specimen fatigue results. The inelastic response of the material at a notch root is treated using Neuber's rule which relates the nominal stresses and strains to the local stresses and strains at the notch root. This is accomplished through the fatigue notch factor (K_f). Necessary parameters in the analysis are depicted in Fig. 22 in which the nominal stress and strain ranges are ΔS and Δe, respectively, while the local stress and strain ranges are $\Delta\sigma$ and $\Delta\epsilon$. Relating these stresses and strains through K_f results in:

$$K_f(\Delta S\ \Delta e\ E)^{\frac{1}{2}} = (\Delta\sigma\ \Delta\epsilon\ E)^{\frac{1}{2}}$$

where K_f = fatigue notch factor

E = modulus of elasticity

Considering cast iron as a notched member (due to the graphite flakes) and the wrought steel with similar structure, hardness and composition as the smooth specimen, a definition of the terms for the Neuber analysis is shown in Fig. 23.

From the constant strain amplitude fatigue tests for the steel, values of the stress and strain range ($\Delta\sigma$ and $\Delta\epsilon$) are registered along with the reversals to failure ($2N_f$). A geometric mean of the product of the stress and strain ranges and the modulus of elasticity is determined (i.e., $(\Delta\sigma\ \Delta\epsilon\ E_s)^{\frac{1}{2}}$). This procedure is repeated for the cast irons, with the concept that the measurements made during the fatigue tests are

nominal stress and strain ranges. The parameter $(\Delta S\ \Delta e\ E_c)^{\frac{1}{2}}$ is developed at the proper life levels.* Results of these calculations for all steels and cast irons are shown in Figs. 24, 25 and 26 where the materials are grouped according to matrix structure. In all instances, the coarser graphite structures again have the lowest fatigue resistance. It should be noted that the curves for the steel, $(\Delta\sigma\ \Delta\epsilon\ E_s)^{\frac{1}{2}}$, and the cast irons, $(\Delta S\ \Delta e\ E_c)^{\frac{1}{2}}$, are essentially parallel after approximately 10^4 reversals. The peculiar shape of these curves for the cast iron results from the difficulty in obtaining a "stabilized" hysteresis loop when testing in the low cycle region as pointed out by Wetzel, et al. (9).

The ratios of the smooth to notched parameters at a given life level determine the fatigue notch factors associated with the various graphite morphologies and matrix structures:

$$K_f = \frac{(\Delta\sigma\ \Delta\epsilon\ E_s)^{\frac{1}{2}}}{(\Delta S\ \Delta e\ E_c)^{\frac{1}{2}}}$$

From these values of K_f, a master plot of $K_f(\Delta S\ \Delta e\ E_c)^{\frac{1}{2}}$ versus $2N_f$ was constructed for the cast irons. Figure 27 shows the results for a constant pearlitic matrix with variable graphite morphology; Fig. 28 shows the results for the martensitic matrix gray irons, while Fig. 29 shows the results for a variable matrix structure (but approximately constant matrix hardness) with mixed graphite structure. Figure 29 again reveals that the matrix structure is not as important as the matrix hardness to the severity of notches. Similar results from steels with varying matrix structures have also been reported by Sinclair and Dolan (10).

---

*The values of ΔS in the case of all cast irons was corrected for area % graphite. Further, E_c is the modulus of elasticity of the cast iron and E_s is the modulus of elasticity of the steel. These were substituted because in the assumption of a nominally elastic response (i.e., $\Delta S = \Delta e\ E_c$) the equation reduces to $K_f\ \Delta S = (\Delta\sigma\ \Delta\epsilon\ E_s)^{\frac{1}{2}}$.

The effectiveness of the graphite flake morphology in decreasing the fatigue resistance of gray iron is summarized in Fig. 30 in which the fatigue notch factor (K_f) versus graphite flake size (ASTM size) is plotted. Similar results were obtained by Ikawa and Ohira (11) for gray irons in which the rotating-bending fatigue limit decreased with increase graphite flake length. It is apparent in Fig. 30 that the value of K_f increases with increase in graphite flake length (i.e., decreasing ASTM size) and with increasing matrix hardness. Values of K_f appear quite large compared to geometric notches such as a plate with a circular hole where the theoretical stress concentration factor (K_t) is a maximum of three under uniaxial loading. However, if the graphite flakes are approximated as elliptical shapes with a length of 0.01 inch and a height of 0.001 inch, values of the theoretical stress concentration factor (K_t) can be obtained as great as 20 for the aspect ratio, $b/a = 10$ (12) as shown in Fig. 31.

Summary and Conclusions

Results have been presented concerning the effect of graphite size, matrix structures and hardness on the fatigue resistance of gray cast iron. Gray iron was considered as a "notched" steel and compared to wrought steels of comparable structure, hardness and composition. A Neuber analysis was employed to assess the effectiveness of graphite flakes as internal "flaws". Quantitative values of the fatigue notch factors (K_f) were obtained for the graphite sizes and matrix structures.

It is concluded that

1. "Bulk" properties do not control the fatigue behavior of gray cast iron.
2. The matrix hardness is of greater importance than the structure (i.e., pearlitic or martensitic of comparable hardness) in determining the fatigue resistance of gray cast iron.

3. Fatigue resistance of gray cast iron is enhanced by decreasing the graphite flake size.
4. Decreasing matrix hardness improves fatigue resistance in the ranges investigated because of a corresponding decrease in "notch sensitivity" with constant graphite morphology.
5. Gray cast iron may be treated as an internally notched steel for determining fatigue resistance.

REFERENCES

1. SAE Fatigue Design Handbook, Vol. 4, Ch. 6, Society of Automotive Engineers, New York, New York, 1968.

2. Mitchell, M. R., "Cyclic Deformation and Fracture Behavior of Gray Cast Iron," M. S. Thesis, Wayne State University, Detroit, Michigan, 1969.

3. Dieter, G. E., Mechanical Metallurgy, Ch. 9, "The Tension Test," McGraw-Hill, New York, p. 242.

4. Landgraf, R. W., Morrow, JoDean, and Endo, T., "Determination of the Cyclic Stress-Strain Curve," ASTM Journal of Materials, JMLSA, Vol. 4, No. 1, March, 1969, pp. 176-199.

5. Landgraf, R. W., "The Resistance of Metals to Cyclic Deformation," Achievement of High Fatigue Resistance in Metals and Alloys, ASTM STP 467, American Society of Testing and Materials, 1970, pp. 3-36.

6. Feltner, C. E. and Mitchell, M. R., "Basic Research on the Cyclic Deformation and Fracture Behavior of Materials," Manual on Low Cyclic Fatigue Testing, ASTM STP 465, American Society for Testing and Materials, 1969, pp. 27-66.

7. Kuhn, P. and Hardrath, H. F., "An Engineering Method for Estimating Notch-Size Effect in Fatigue Tests on Steel," NACA, Tech. Note 2805, October, 1952.

8. Topper, T. H., Wetzel, R. M., and Morrow, JoDean, "Neuber's Rule Applied to Fatigue of Notched Specimens," ASTM Journal of Materials, JMLSA, Vol. 4, No. 1, March, 1969, pp. 200-209.

9. Wetzel, R. M., Morrow, JoDean, and Topper, T. H., "Fatigue of Notched Parts with Emphasis on Local Stresses and Strains," Naval Air Development Center Report No. NADC-ST-6818, September, 1968.

10. Sinclair, G. M. and Dolan, T. J., "Some Effects of Austenitic Grain Size and Metallurgical Structure on the Mechanical Properties of Steel," ASTM Proc., Vol. 50, 1950, pp. 587-618.

11. Ikawa, K. and Ohira, G., "Fatigue Properties of Cast Iron in Relation to Graphite Structure," AFS Cast Metals Research Journal, Vol. 3, No. 1, March, 1967, pp. 11-21.

12. Peterson, R. E., Stress Concentration Design Factors, Wiley & Sons, Inc., New York, New York, 1953, p. 88, see also Stress Concentration Factors, Wiley & Sons, Inc., New York, New York, 1974, p. 195.

TABLE 1 - COMPOSITION OF GRAY CAST IRONS AND STEEL

	Gray Irons	Steel
w/o C[+]	3.30	0.61
w/o Mn	0.85	0.78
w/o Si	1.94	1.95
w/o S	0.10	0.01
w/o P	0.02	0.01
w/o Cr	0.29	0.25
w/o C. C.*	0.62	---
C. E.**	3.89	---

[+]For the gray irons this represents total carbon which includes both graphitic and combined carbon.

*C. C. ≡ Combined Carbon

**C. E. ≡ Carbon Equivalent ≡ w/o C + $\frac{1}{3}$ w/o Si - $\frac{1}{3}$ (w/o Cr - 0.1)

TABLE 2 - MONOTONIC AND CYCLIC STRESS-STRAIN PROPERTIES FOR SAE 9262 STEEL AT 272 DPH, PEARLITIC MATRIX

Monotonic Tension Properties:	
Modulus of Elasticity, E	30×10^3 ksi
Yield Strength, 0.2% S_y	66 ksi
Ultimate Strength, S_u	134 ksi
Red. in Area, % RA	14
True Fracture Strength, σ_f	151 ksi
True Fracture Ductility, ϵ_f	0.16
Strain Hardening Exponent, n	0.22
Strength Coefficient, K	253 ksi
True Toughness, U_p	19.7 ksi
Cyclic Properties:	
Yield Strength, 0.2% S_y'	76 ksi
Strain Hardening Exponent, n'	0.15
Strength Coefficient, K'	200 ksi
Fatigue Strength Coefficient, σ_f'	151 ksi
Fatigue Ductility Coefficient, ϵ_f'	0.155
Fatigue Strength Exponent, b	-0.071
Fatigue Ductility Exponent, c	-0.47
Transition Fatigue Life, $2N_t$	5,200 rev

TABLE 3 - MONOTONIC AND CYCLIC STRESS-STRAIN PROPERTIES FOR SAE 9262 STEEL AT 286 DPH, MARTENSITIC MATRIX

Monotonic Tension Properties:	
Modulus of Elasticity, E	28×10^3 ksi
Yield Strength, 0.2% S_y	114 ksi
Ultimate Strength, S_u	145 ksi
Red. in Area, % RA	33
True Fracture Strength, σ_f	177 ksi
True Fracture Ductility, ϵ_f	0.41
Strain Hardening Exponent, n	0.14
Strength Coefficient, K	216 ksi
True Toughness, U_p	63.5 ksi
Cyclic Properties:	
Yield Strength, 0.2% S_y'	94 ksi
Strain Hardening Exponent, n'	0.12
Strength Coefficient, K'	197 ksi
Fatigue Strength Coefficient, σ_f'	177 ksi
Fatigue Ductility Coefficient, ϵ_f'	0.41
Fatigue Strength Exponent, b	-0.073
Fatigue Ductility Exponent, c	-0.60
Transition Fatigue Life, $2N_t$	3,000 rev

TABLE 4 - MONOTONIC AND CYCLIC STRESS-STRAIN PROPERTIES FOR SAE 9262 STEEL AT 434 DPH, MARTENSITIC MATRIX

Monotonic Tension Properties:	
Modulus of Elasticity, E	29×10^3 ksi
Yield Strength, 0.2% S_y	200 ksi
Ultimate Strength, S_u	227 ksi
Red. in Area, % RA	32
True Fracture Strength, σ_f	269 ksi
True Fracture Ductility, ϵ_f	0.38
Strain Hardening Exponent, n	0.06
Strength Coefficient, K	283 ksi
True Toughness, U_p	99.3 ksi
Cyclic Properties:	
Yield Strength, 0.2% S_y'	152 ksi
Strain Hardening Exponent, n'	0.089
Strength Coefficient, K'	292 ksi
Fatigue Strength Coefficient, σ_f'	269 ksi
Fatigue Ductility Coefficient, ϵ_f'	0.38
Fatigue Strength Exponent, b	-0.057
Fatigue Ductility Exponent, c	-0.65
Transition Fatigue Life, $2N_t$	620 rev

TABLE 5 - STRAIN-LIFE RESULTS FOR SAE 9262 STEEL

Strain Amplitude $\Delta\epsilon/2$	Plastic Strain $\Delta\epsilon_p/2$	Elastic Strain $\Delta\epsilon_e/2$	Reversals to Failure $2N_f$
Pearlitic Matrix at 272 DPH:			
0.0170	0.0135	0.0035	414
0.0070	0.0040	0.0030	2,660
0.0030	0.0024	0.0006	40,600
Martensitic Matrix at 434 DPH:			
0.0180	0.0110	0.0070	304
0.0060	0.0010	0.0050	7,180
0.0030	---	$\approx$0.0030	8.4×10^{6}*
Martensitic Matrix at 286 DPH:			
0.0180	0.0135	0.0045	400
0.0060	0.0026	0.0034	5,600
0.0030	0.0003	0.0027	1.13×10^{5}

*Test stopped--specimen did not fail.

TABLE 6 - MONOTONIC STRESS-STRAIN PROPERTIES OF PEARLITIC GRAY CAST IRON WITH MATRIX HARDNESS OF 272 DPH. GRAPHITE SIZE ASTM 3-4, TYPE A (COARSE)

	Tension/Compression
Modulus of Elasticity, E	$14.5/15.4 \times 10^3$ ksi
Yield Strength, 0.2% S_y	25/44 ksi
Ultimate Strength, S_u	28/90 ksi
Red. in Area, % RA	nil.
True Fracture Strength, σ_f	28/-- ksi
True Fracture Ductility, ϵ_f	0.006/---
Strain Hardening Exponent, n	0.21/0.25
Strength Coefficient, K	93/187 ksi
True Toughness, U_p	0.13 ksi

TABLE 7 - MONOTONIC STRESS-STRAIN PROPERTIES OF PEARLITIC GRAY CAST IRON AT MATRIX HARDNESS OF 272 DPH. GRAPHITE SIZE 50% ASTM 4-5, 50% ASTM 7, TYPE A (FINE)

	Tension/Compression
Modulus of Elasticity, E	16.3/16.7 x 10^3 ksi
Yield Strength, 0.2% S_y	33/61 ksi
Ultimate Strength, S_u	40/120 ksi
Red. in Area, % RA	nil.
True Fracture Strength, σ_f	40/-- ksi
True Fracture Ductility, ϵ_f	0.008/---
Strain Hardening Exponent, n	0.23/0.24
Strength Coefficient, K	135/243 ksi
True Toughness, U_p	0.26 ksi

TABLE 8 - MONOTONIC STRESS-STRAIN PROPERTIES OF PEARLITIC GRAY CAST IRON WITH MATRIX HARDNESS OF 272 DPH. GRAPHITE SIZE 60% ASTM 4-5, TYPE A; 40% TYPE D (MIXED)

	Tension/Compression
Modulus of Elasticity, E	15.2/16.5 x 10^3 ksi
Yield Strength, 0.2% S_y	32/63 ksi
Ultimate Strength, S_u	38/126
Red. in Area, % RA	nil.
True Fracture Strength, σ_f	41/-- ksi
True Fracture Ductility, ϵ_f	0.007/---
Strain Hardening Exponent, n	0.19/0.18
Strength Coefficient, K	104/197 ksi
True Toughness, U_p	0.25 ksi

TABLE 9 - MONOTONIC STRESS-STRAIN PROPERTIES OF MARTENSITIC GRAY CAST IRON WITH MATRIX HARDNESS OF 434 DPH.
GRAPHITE SIZE ASTM 3-4, TYPE A (COARSE)

	Tension/Compression
Modulus of Elasticity, E	11.9/11.2 x 10^3 ksi
Yield Strength, 0.2% S_y	---/190 ksi
Ultimate Strength, S_u	36/200
Red. in Area, % RA	nil.
True Fracture Strength, σ_f	36/-- ksi
True Fracture Ductility, ϵ_f	0.004/---
Strain Hardening Exponent, n	---
Strength Coefficient, K	--- ksi
True Toughness, U_p	--- ksi

TABLE 10 - MONOTONIC STRESS-STRAIN PROPERTIES OF MARTENSITIC GRAY CAST IRON WITH MATRIX HARDNESS OF 434 DPH. GRAPHITE SIZE 50% ASTM 4-5, 50% ASTM 7, TYPE A (FINE)

	Tension/Compression
Modulus of Elasticity, E	$12.3/12.4 \times 10^3$ ksi
Yield Strength, 0.2% S_y	---/220 ksi
Ultimate Strength, S_u	53/230
Red. in Area, % RA	nil.
True Fracture Strength, σ_f	53/-- ksi
True Fracture Ductility, ϵ_f	---
Strain Hardening Exponent, n	---
Strength Coefficient, K	--- ksi
True Toughness, U_p	--- ksi

TABLE 11 - MONOTONIC STRESS-STRAIN PROPERTIES OF MARTENSITIC GRAY CAST IRON WITH MATRIX HARDNESS OF 434 DPH. GRAPHITE SIZE 60% ASTM 4-5, TYPE A; 40% TYPE D (MIXED)

	Tension/Compression
Modulus of Elasticity, E	13.8/16.2 x 10^3 ksi
Yield Strength, 0.2% S_y	---/260 ksi
Ultimate Strength, S_u	63/265
Red. in Area, % RA	nil.
True Fracture Strength, σ_f	63/-- ksi
True Fracture Ductility, ϵ_f	0.005/---
Strain Hardening Exponent, n	---
Strength Coefficient, K	--- ksi
True Toughness, U_p	--- ksi

TABLE 12 - MONOTONIC STRESS-STRAIN PROPERTIES OF MARTENSITIC GRAY CAST IRON WITH MATRIX HARDNESS OF 286 DPH. GRAPHITE SIZE 60% ASTM 4-5, TYPE A; 40% TYPE D (MIXED)

	Tension/Compression
Modulus of Elasticity, E	13.7/14.1 x 10^3 ksi
Yield Strength, 0.2% S_y	41/60 ksi
Ultimate Strength, S_u	43/134
Red. in Area, % RA	nil.
True Fracture Strength, σ_f	43/-- ksi
True Fracture Ductility, ϵ_f	0.006/---
Strain Hardening Exponent, n	0.22/0.24
Strength Coefficient, K	165/304 ksi
True Toughness, U_p	0.21 ksi

TABLE 13 - STRAIN-LIFE FATIGUE RESULTS OF PEARLITIC MATRIX GRAY CAST IRON (272 DPH) WITH VARYING GRAPHITE MORPHOLOGY

Strain Amplitude $\Delta\epsilon/2$	Reversals to Failure $2N_f$
Coarse Graphite:	
0.0035	110
0.0018	3,800
0.0011	24,000
0.0008	1.3×10^5
0.0005	$2.0 \times 10^{7*}$
Fine Graphite:	
0.0048	72
0.0024	2,800
0.0016	13,000
0.0012	1.9×10^5
0.0008	$4.5 \times 10^{7*}$
Mixed Graphite:	
0.0050	20
0.0035	170
0.0024	1,800
0.0016	39,000
0.0013	2.5×10^5
0.0010	$2.0 \times 10^{7*}$

*Test stopped--specimen did not fail.

TABLE 14 - STRAIN-LIFE FATIGUE RESULTS OF MARTENSITIC MATRIX GRAY CAST IRON (434 DPH) WITH VARYING GRAPHITE MORPHOLOGY

Strain Amplitude $\Delta\epsilon/2$	Reversals to Failure $2N_f$
Coarse Graphite:	
0.0024	900
0.0010	75,000
0.0007	6.5×10^5
0.0005	$1.0 \times 10^{8*}$
Fine Graphite:	
0.0032	580
0.0015	45,000
0.0008	5.8×10^5
0.0006	$1.0 \times 10^{8*}$
Mixed Graphite:	
0.0030	150
0.0015	50,000
0.0008	1.1×10^6
0.0006	8.0×10^6

*Test stopped--specimen did not fail.

TABLE 15 - STRAIN-LIFE FATIGUE RESULTS OF MARTENSITIC MATRIX GRAY CAST IRON (286 DPH) WITH MIXED GRAPHITE MORPHOLOGY

Strain Amplitude $\Delta\epsilon/2$	Reversals to Failure $2N_f$
0.0036	32
0.0027	280
0.0020	6,500
0.0016	13,000

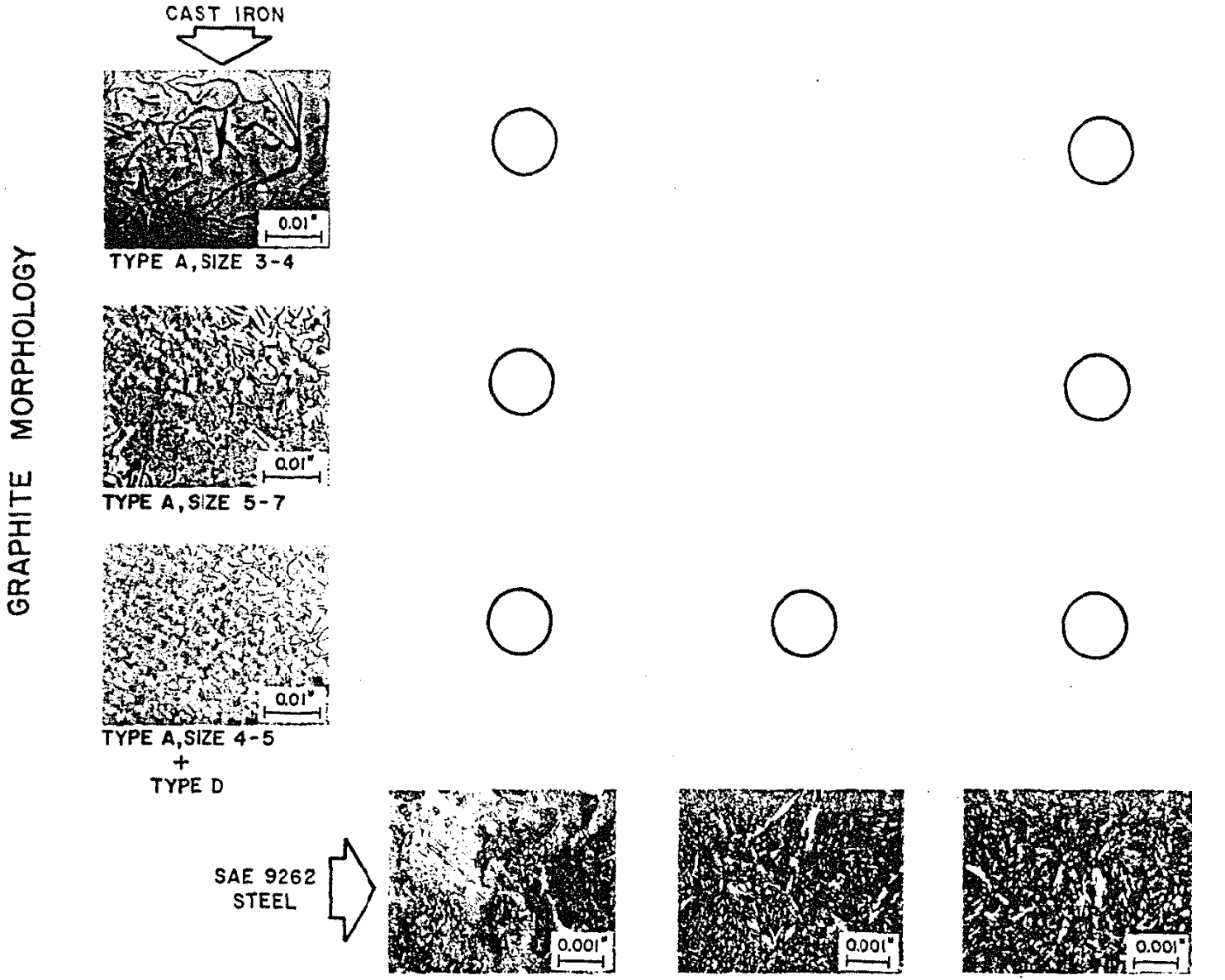

FIG. 1 GRAPHITE MORPHOLOGIES AND MATRIX STRUCTURES OF CAST IRONS AND STEELS

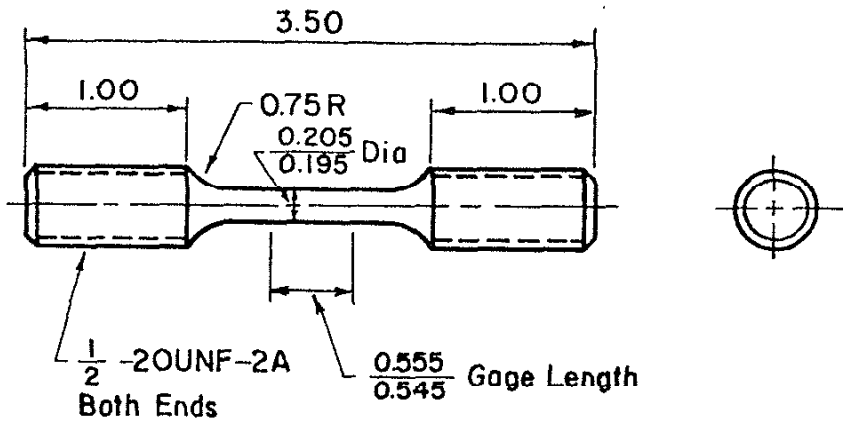

FIG. 2 SPECIMEN DESIGN FOR SAE 9262 STEEL

COARSE

ASTM TYPE A
SIZE 3-4

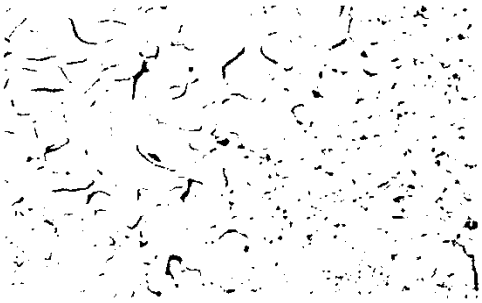

FINE

ASTM TYPE A
SIZE 5-7

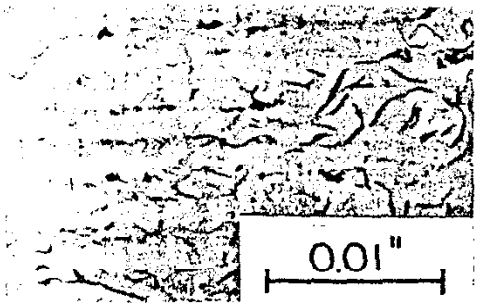

MIXED

60% ASTM TYPE A
SIZE 4-5

40% ASTM TYPE D

UNETCHED

PICRAL ETCHED

FIG. 3 MICROGRAPHS OF GRAY CAST IRON GRAPHITE MORPHOLOGY AND AS-CAST PEARLITIC MATRIX STRUCTURES

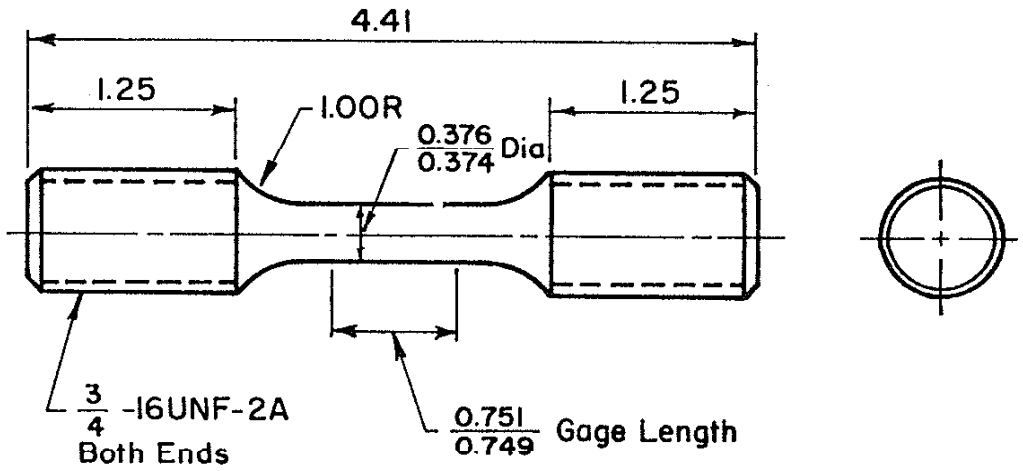

FIG. 4 SPECIMEN DESIGN FOR GRAY CAST IRONS

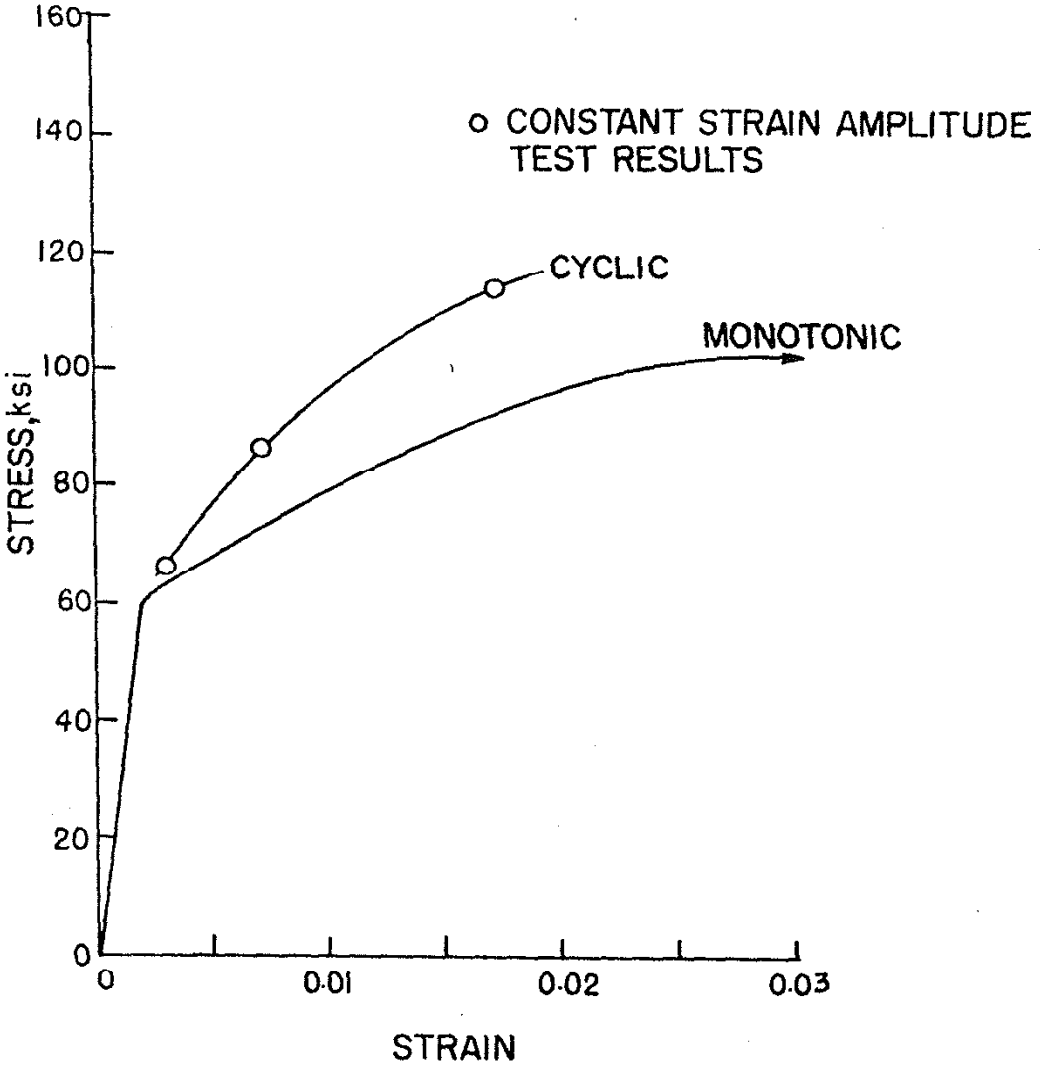

FIG. 5 MONOTONIC AND CYCLIC STRESS-STRAIN CURVES FOR SAE 9262 STEEL, PEARLITIC MATRIX AT 272 DPH

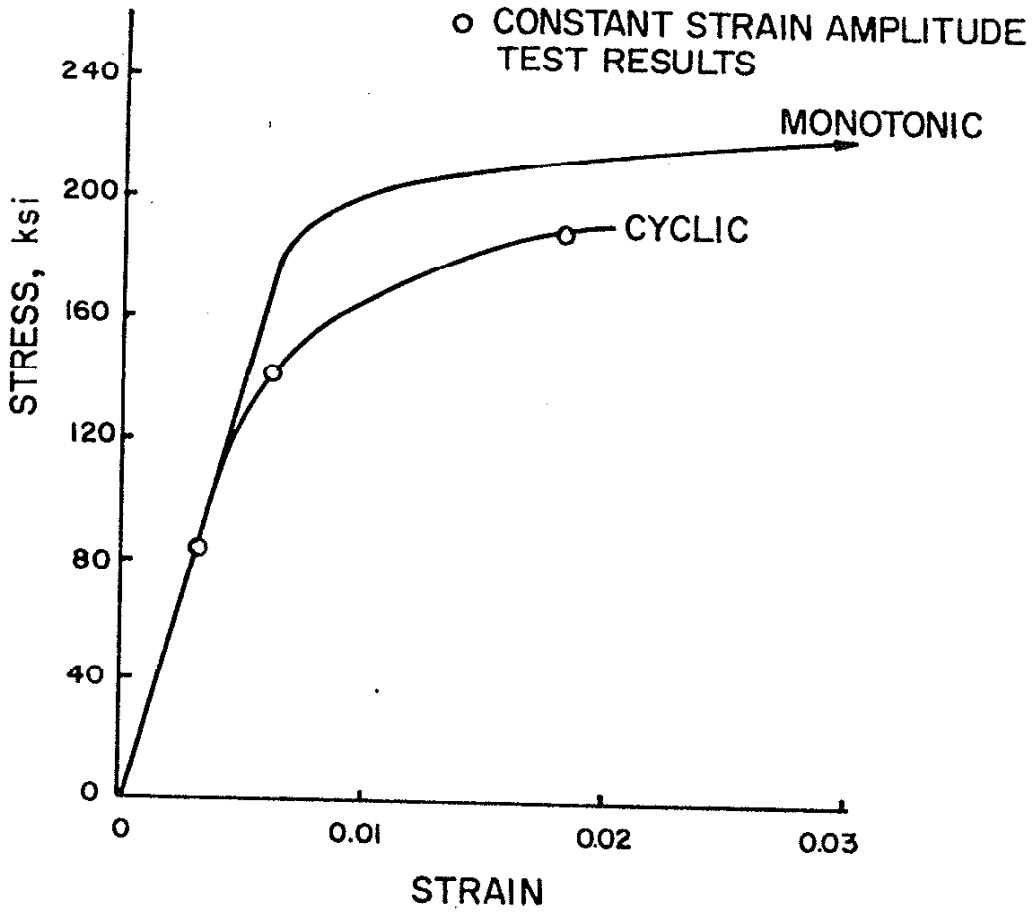

FIG. 6 MONOTONIC AND CYCLIC STRESS-STRAIN CURVES FOR SAE 9262 STEEL, MARTENSITIC MATRIX AT 434 DPH

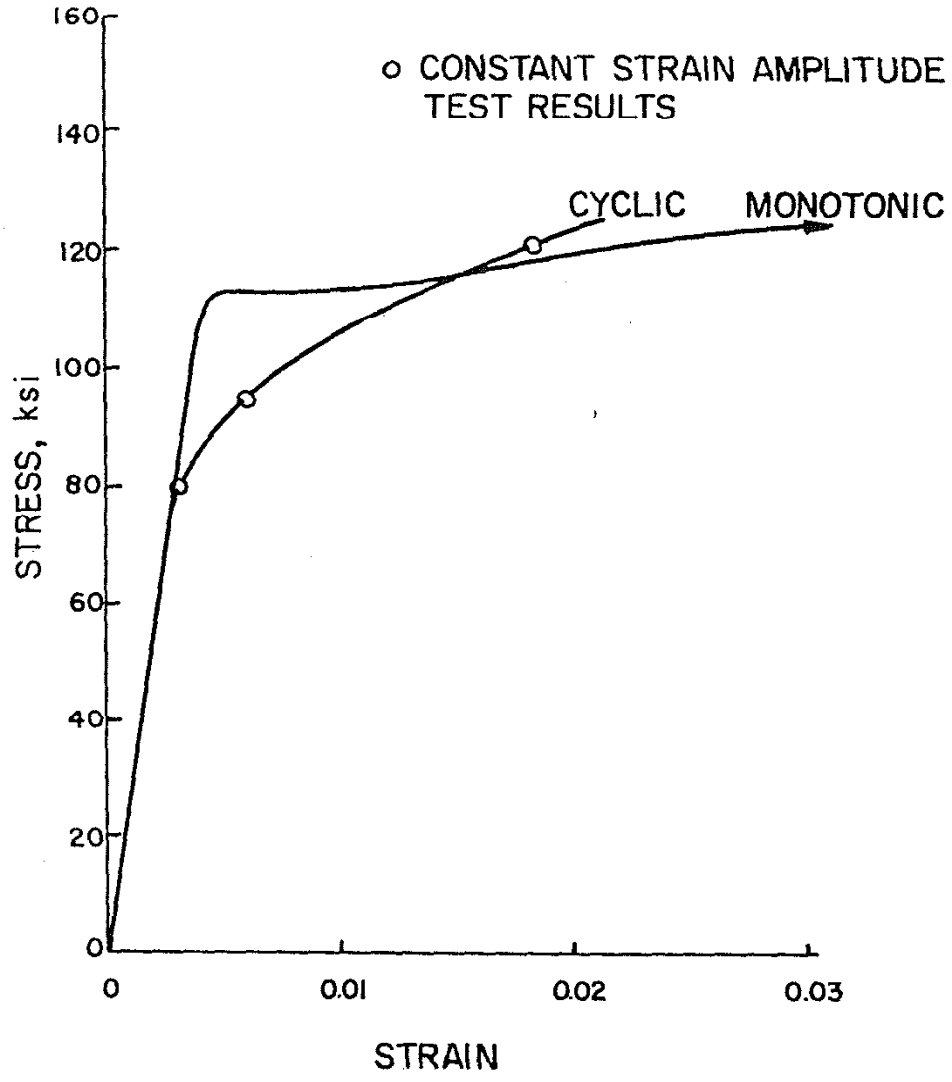

FIG. 7 MONOTONIC AND CYCLIC STRESS-STRAIN CURVES FOR SAE 9262 STEEL, MARTENSITIC MATRIX AT 286 DPH

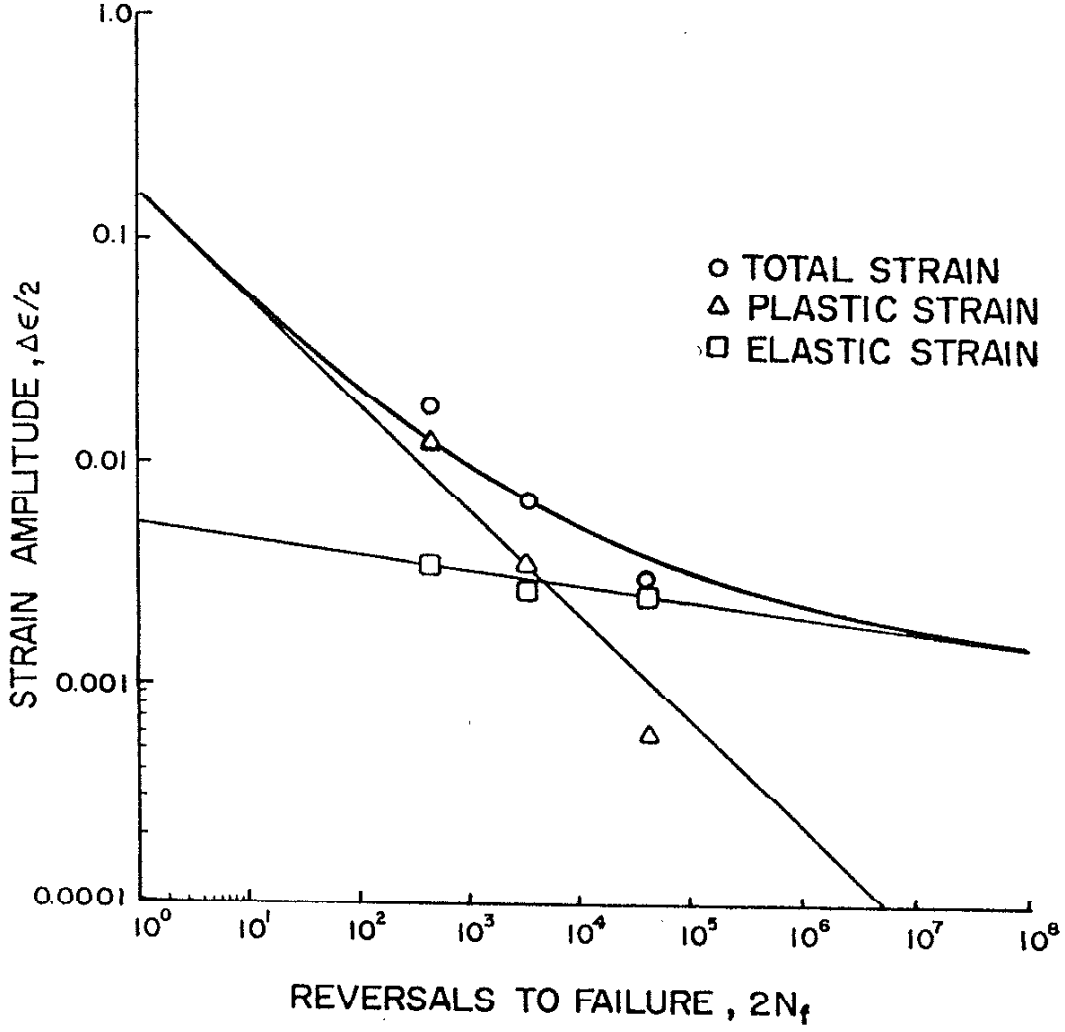

FIG. 8 STRAIN AMPLITUDE VS. REVERSALS TO FAILURE CURVE FOR SAE 9262 STEEL, PEARLITIC MATRIX AT 272 DPH

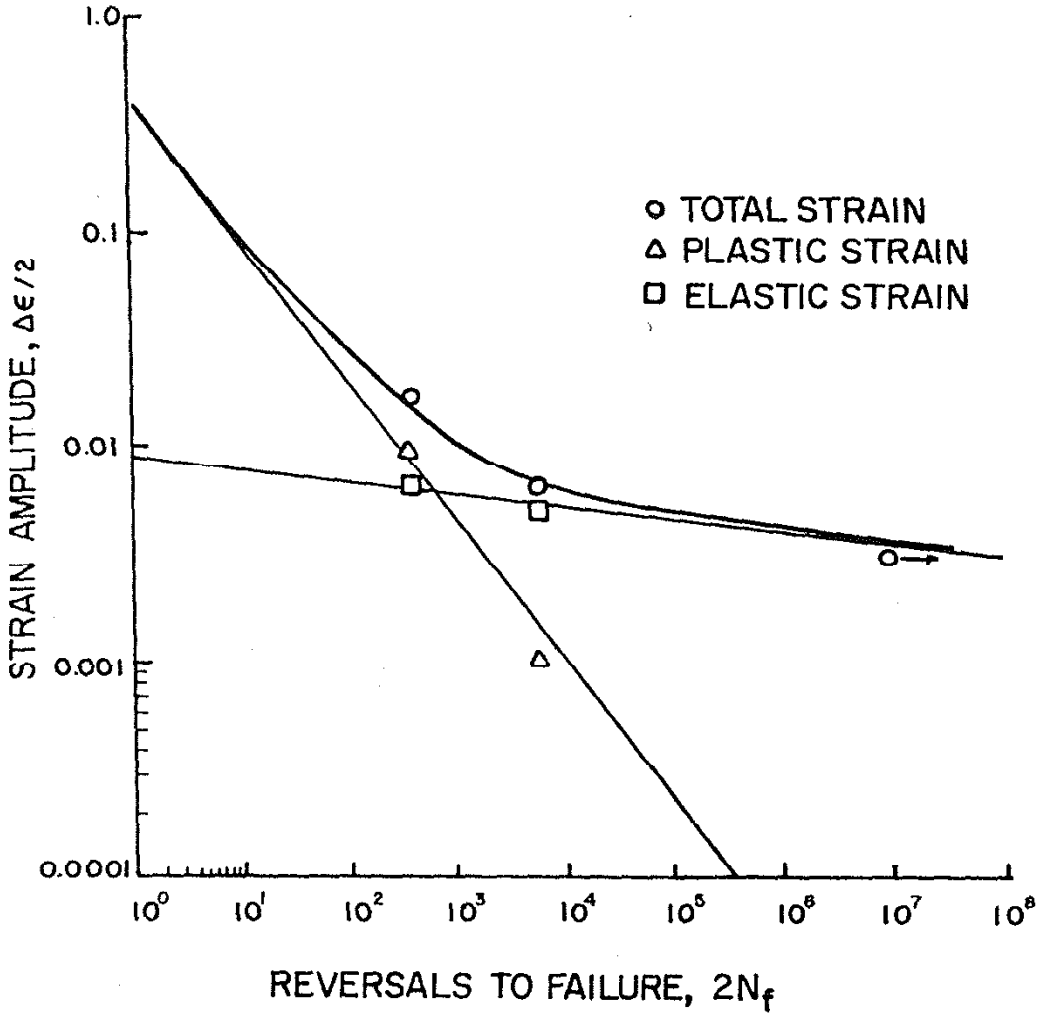

FIG. 9 STRAIN AMPLITUDE VS. REVERSALS TO FAILURE CURVE FOR SAE 9262 STEEL, MARTENSITIC MATRIX AT 434 DPH

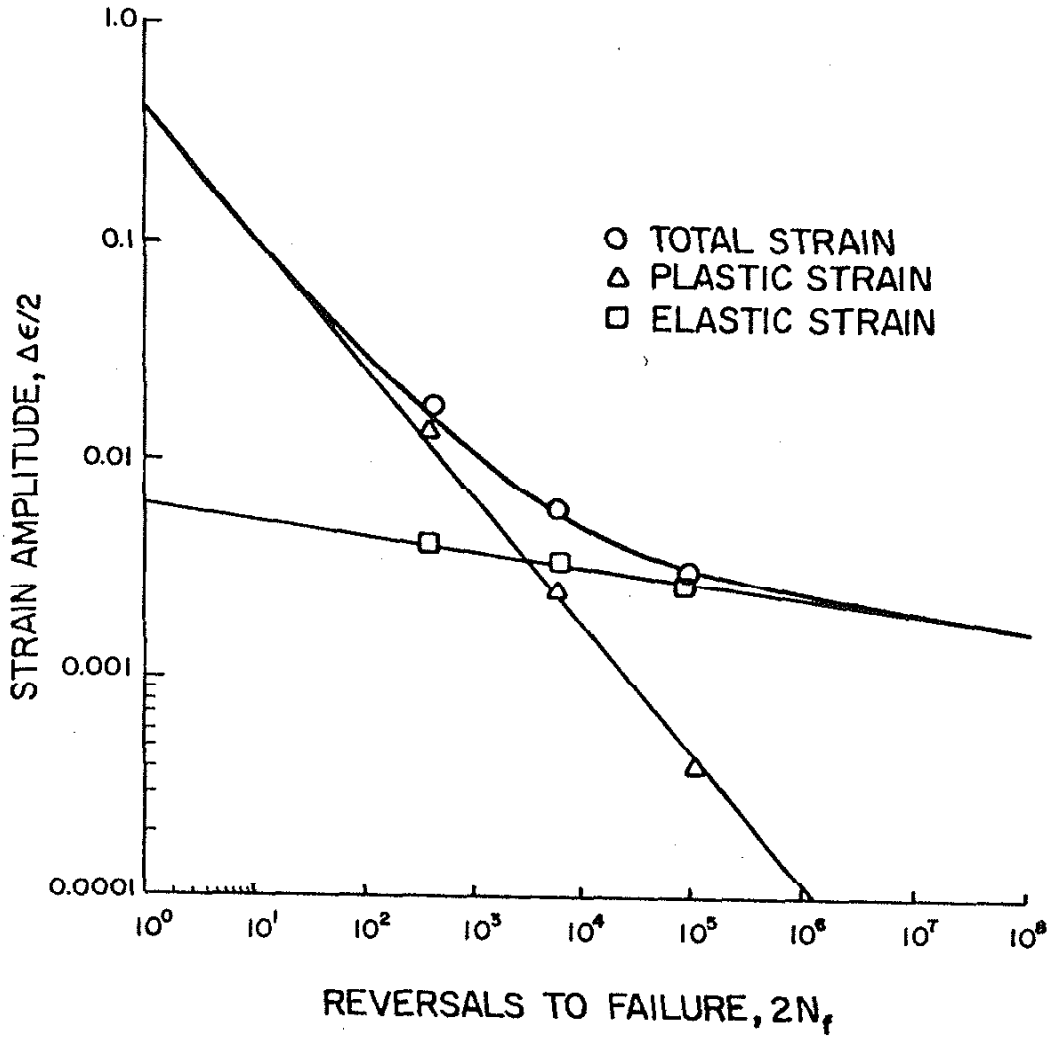

FIG. 10 STRAIN AMPLITUDE VS. REVERSALS TO FAILURE CURVE FOR SAE 9262 STEEL, MARTENSITIC MATRIX AT 286 DPH

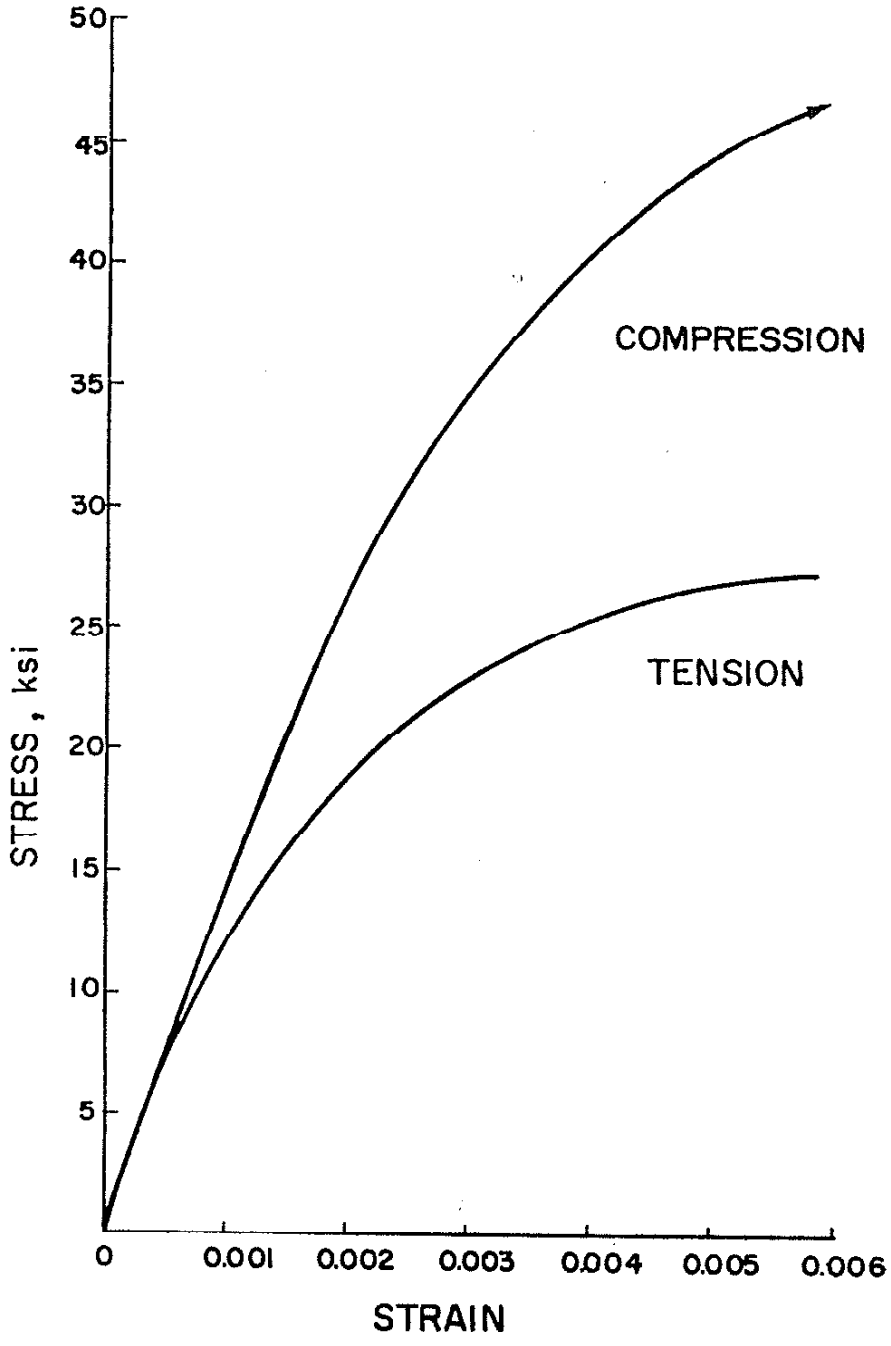

FIG. 11 MONOTONIC TENSION AND COMPRESSION STRESS-STRAIN CURVES FOR PEARLITIC MATRIX GRAY CAST IRON (272 DPH) WITH COARSE GRAPHITE

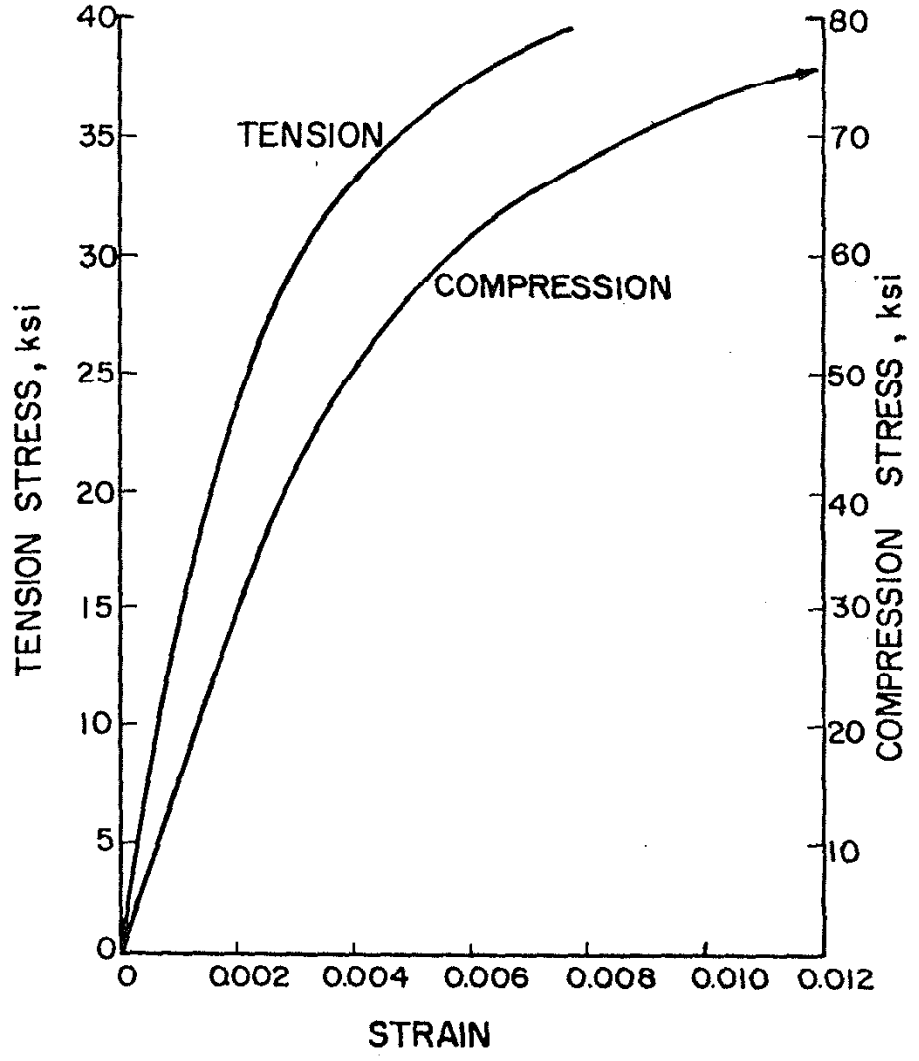

FIG. 12 MONOTONIC TENSION AND COMPRESSION STRESS-STRAIN CURVES FOR PEARLITIC MATRIX GRAY CAST IRON (272 DPH) WITH FINE GRAPHITE

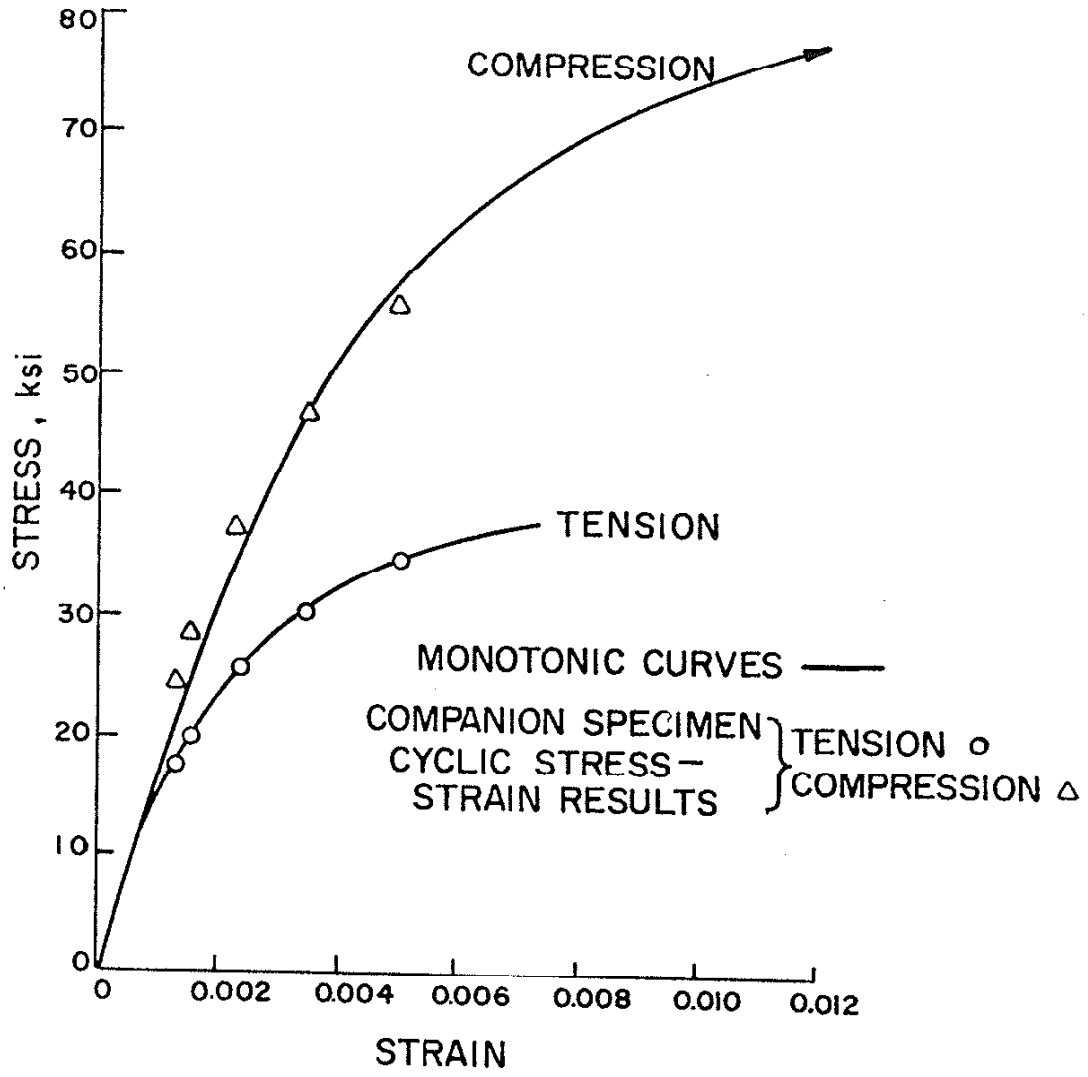

FIG. 13 MONOTONIC TENSION AND COMPRESSION STRESS-STRAIN CURVES AND CYCLIC STRESS-STRAIN CURVES FOR PEARLITIC MATRIX GRAY CAST (272 DPH) WITH MIXED GRAPHITE

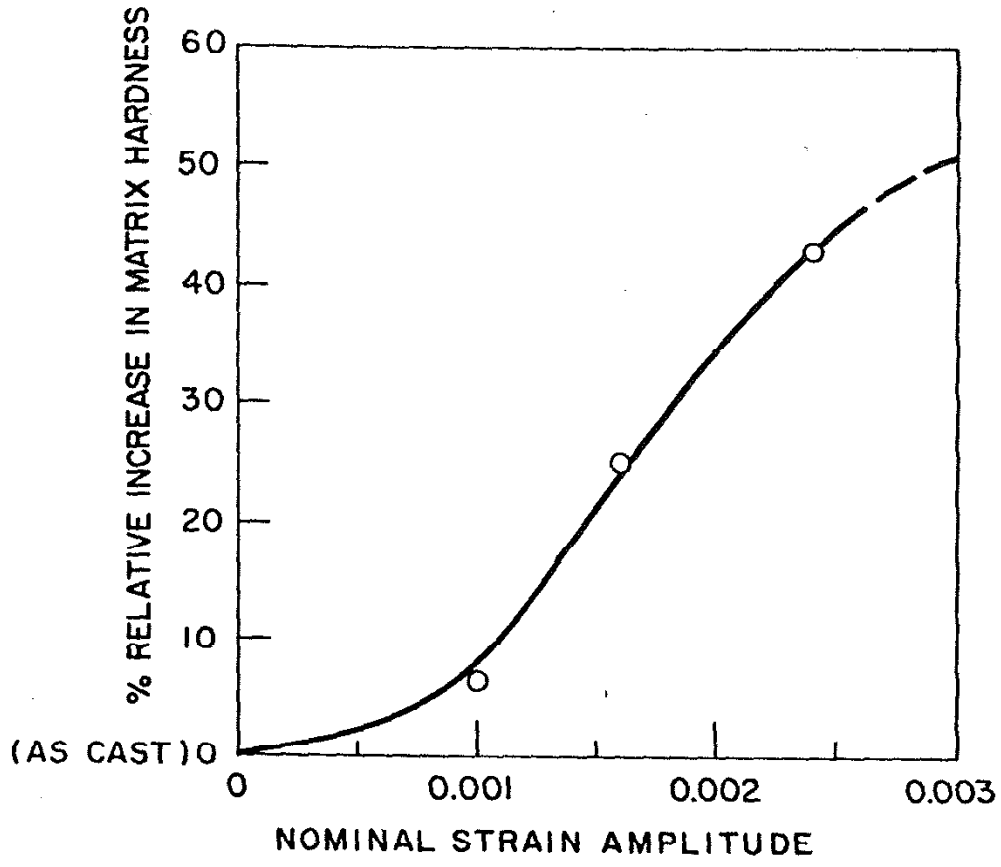

FIG. 14 RELATIVE INCREASE IN MATRIX HARDNESS VS. NOMINAL STRAIN AMPLITUDE FOR PEARLITIC GRAY CAST IRON WITH MIXED GRAPHITE

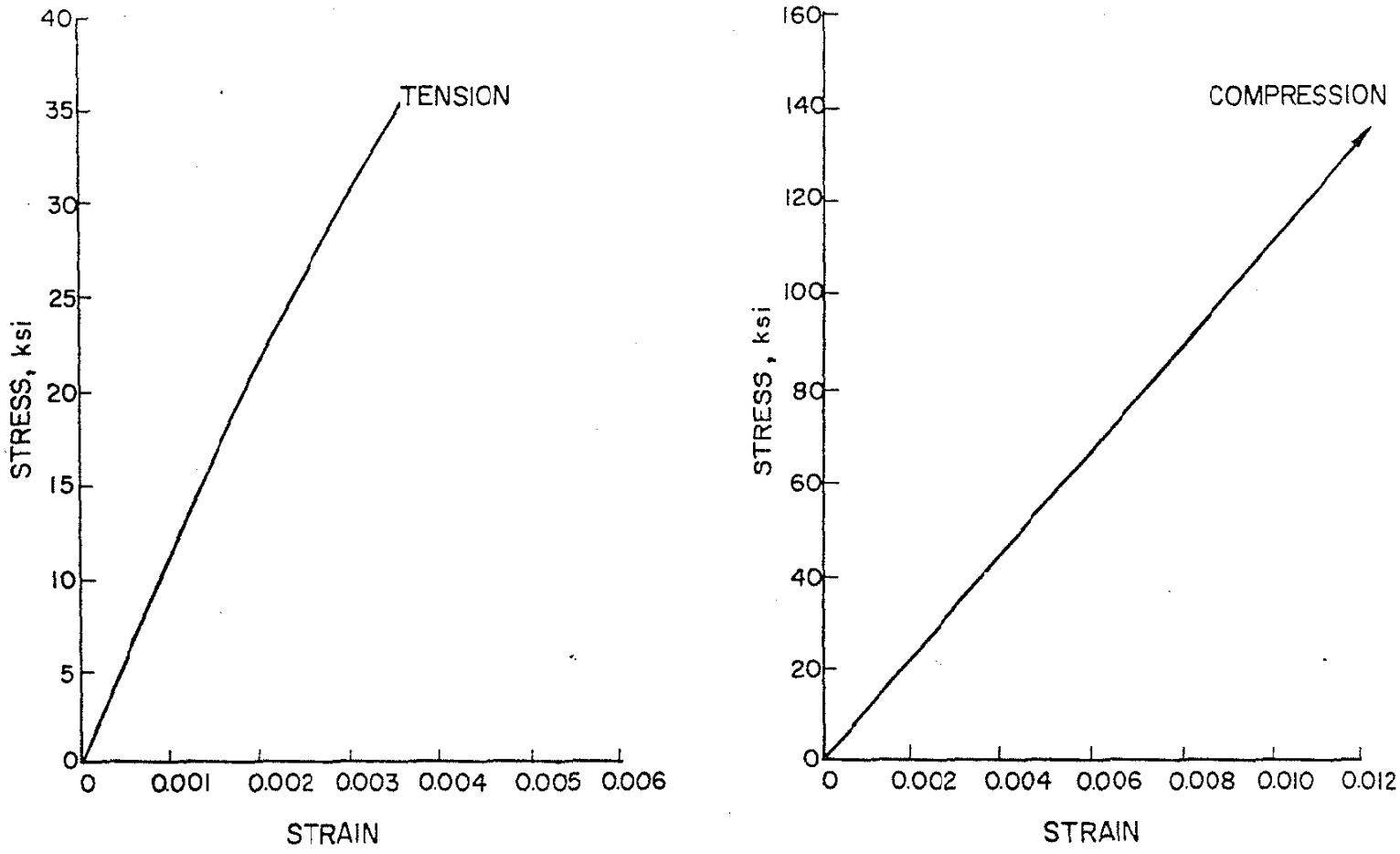

FIG. 15 MONOTONIC STRESS-STRAIN CURVES FOR MARTENSITIC MATRIX GRAY CAST IRON (434 DPH) WITH COARSE GRAPHITE

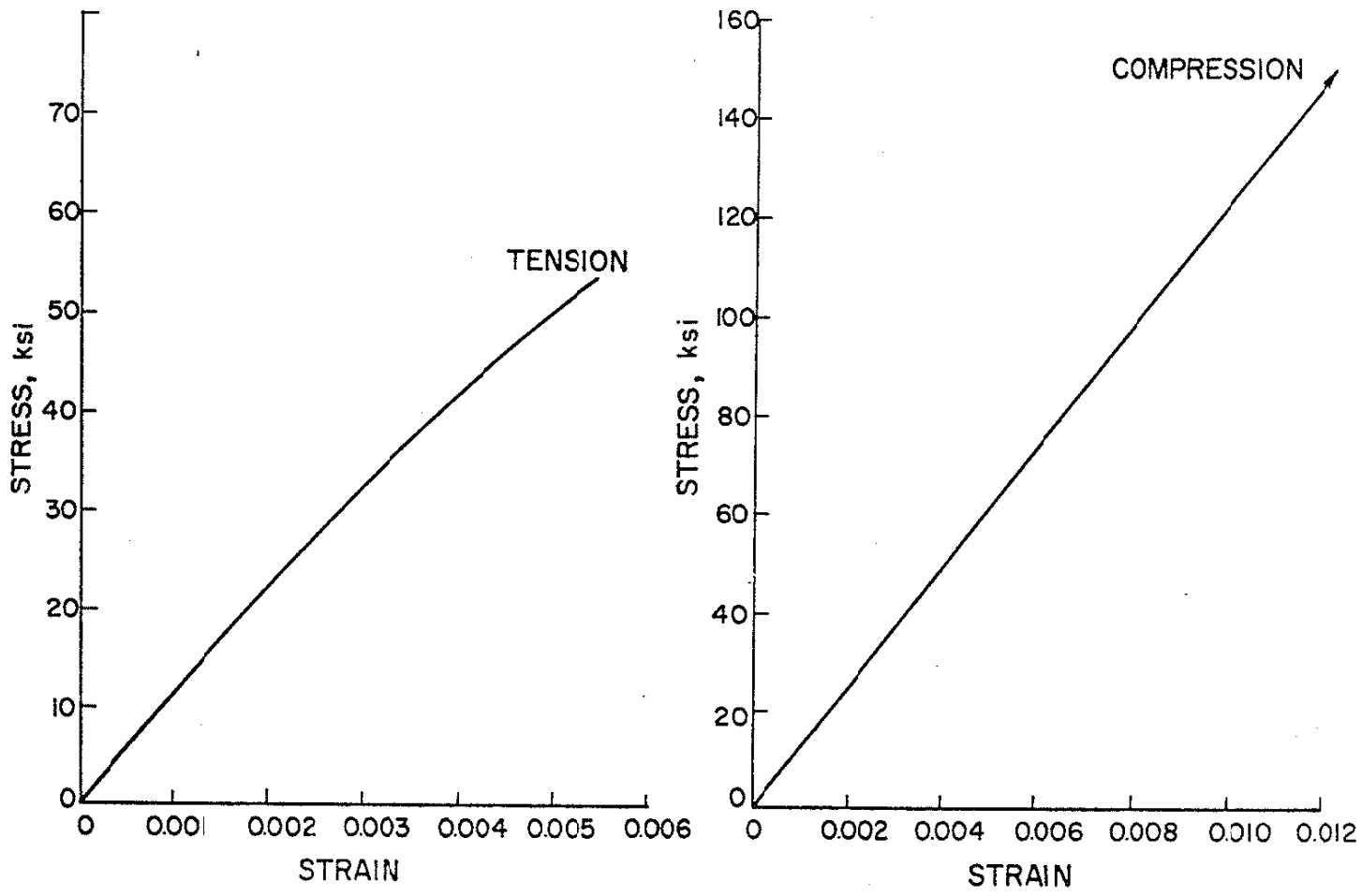

FIG. 16 MONOTONIC STRESS-STRAIN CURVES FOR MARTENSITIC MATRIX GRAY CAST IRON (434 DPH) WITH FINE GRAPHITE

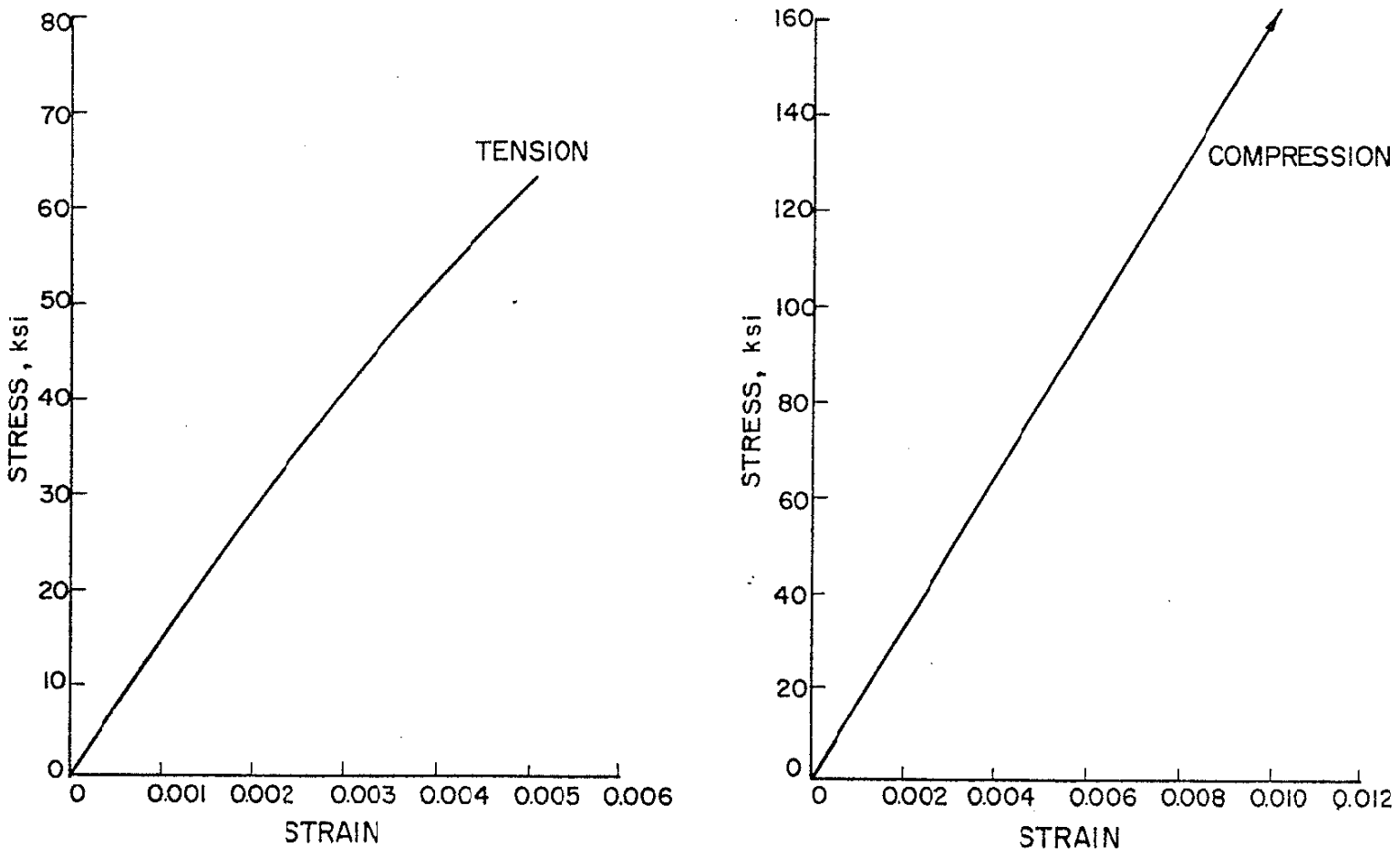

FIG. 17 MONOTONIC STRESS-STRAIN CURVES FOR MARTENSITIC MATRIX GRAY CAST IRON (434 DPH) WITH MIXED GRAPHITE

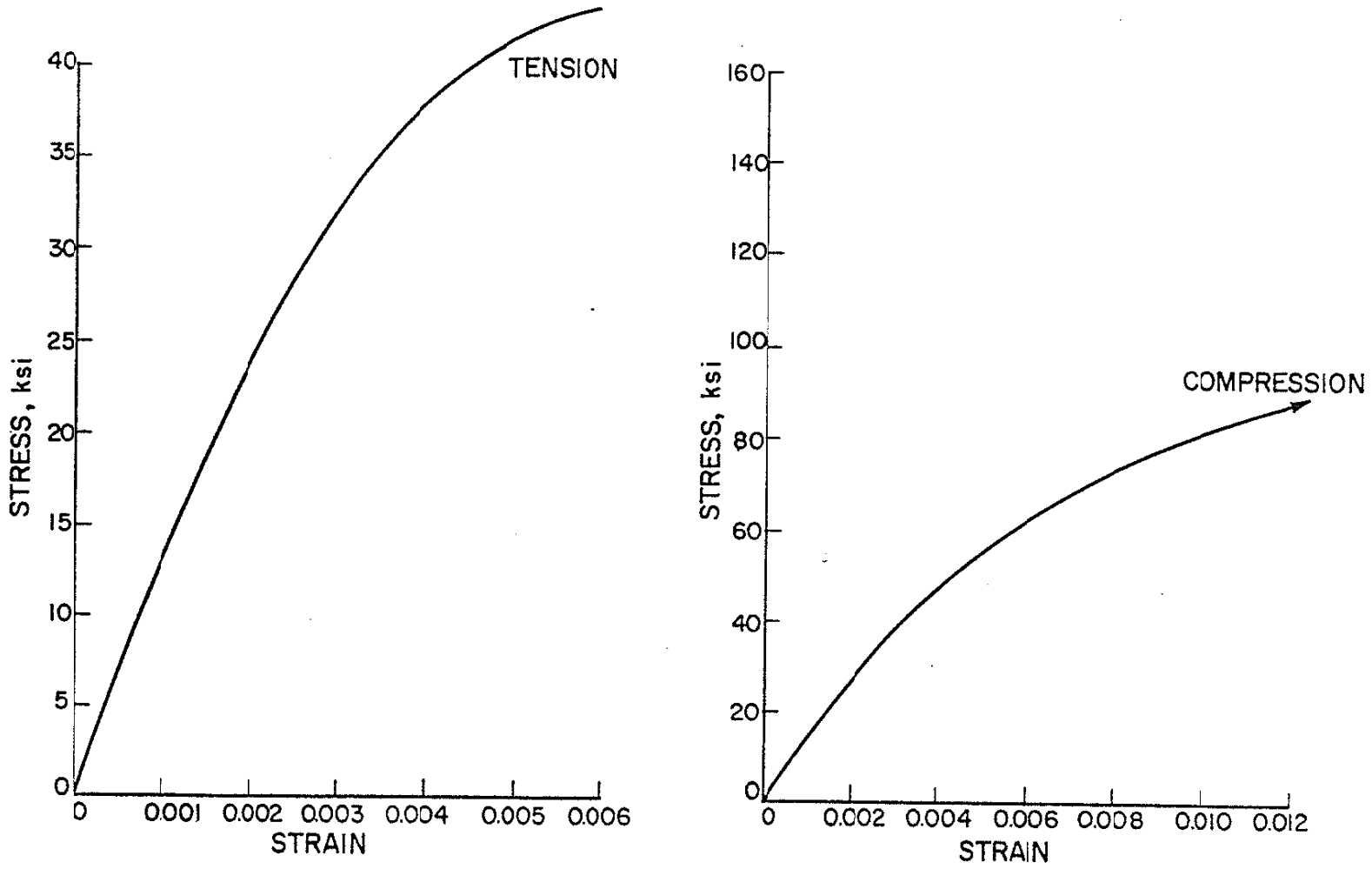

FIG. 18 MONOTONIC STRESS-STRAIN CURVES FOR MARTENSITIC MATRIX GRAY CAST IRON (286 DPH) WITH MIXED GRAPHITE

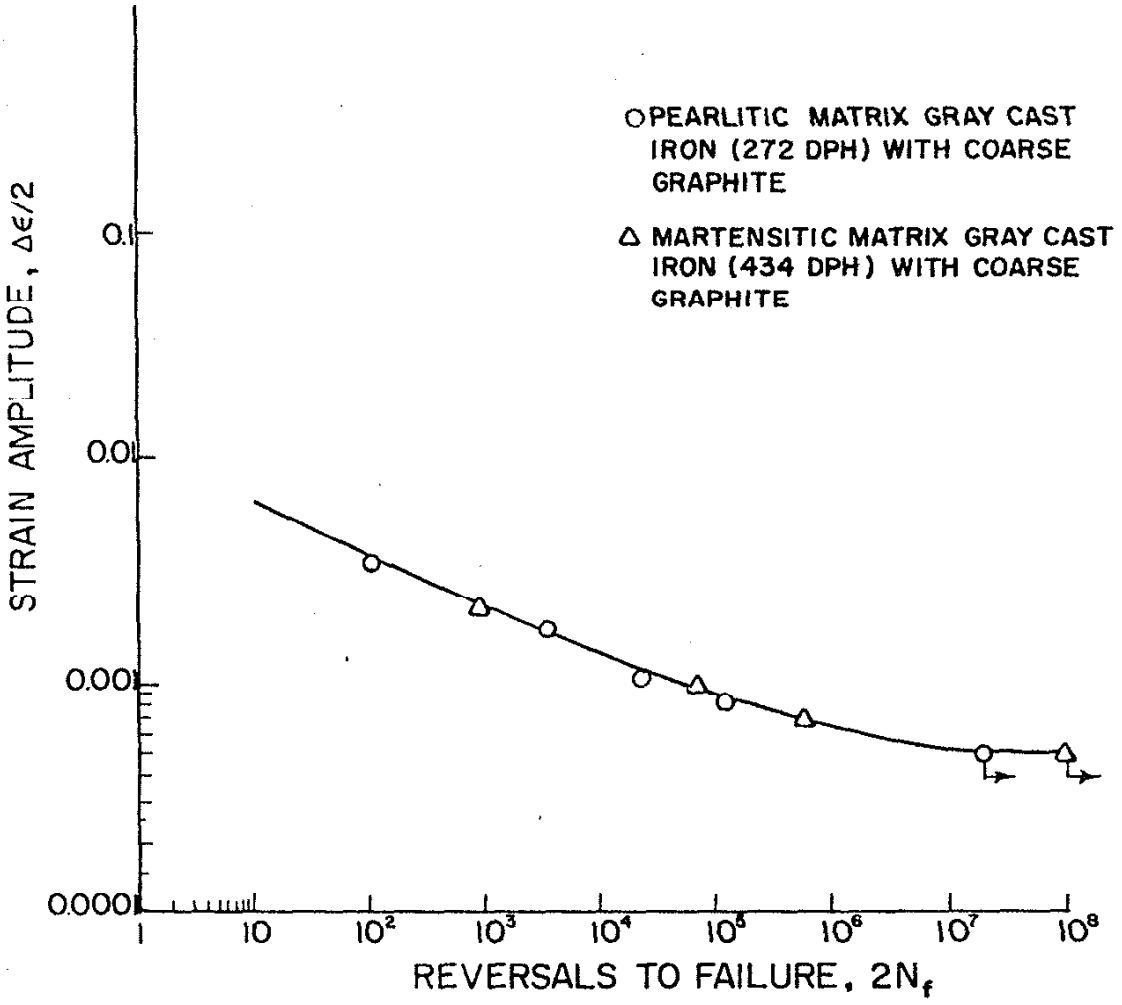

FIG. 19 STRAIN-LIFE CURVE FOR PEARLITIC (272 DPH) AND MARTENSITIC (434 DPH) GRAY CAST IRON WITH COARSE GRAPHITE

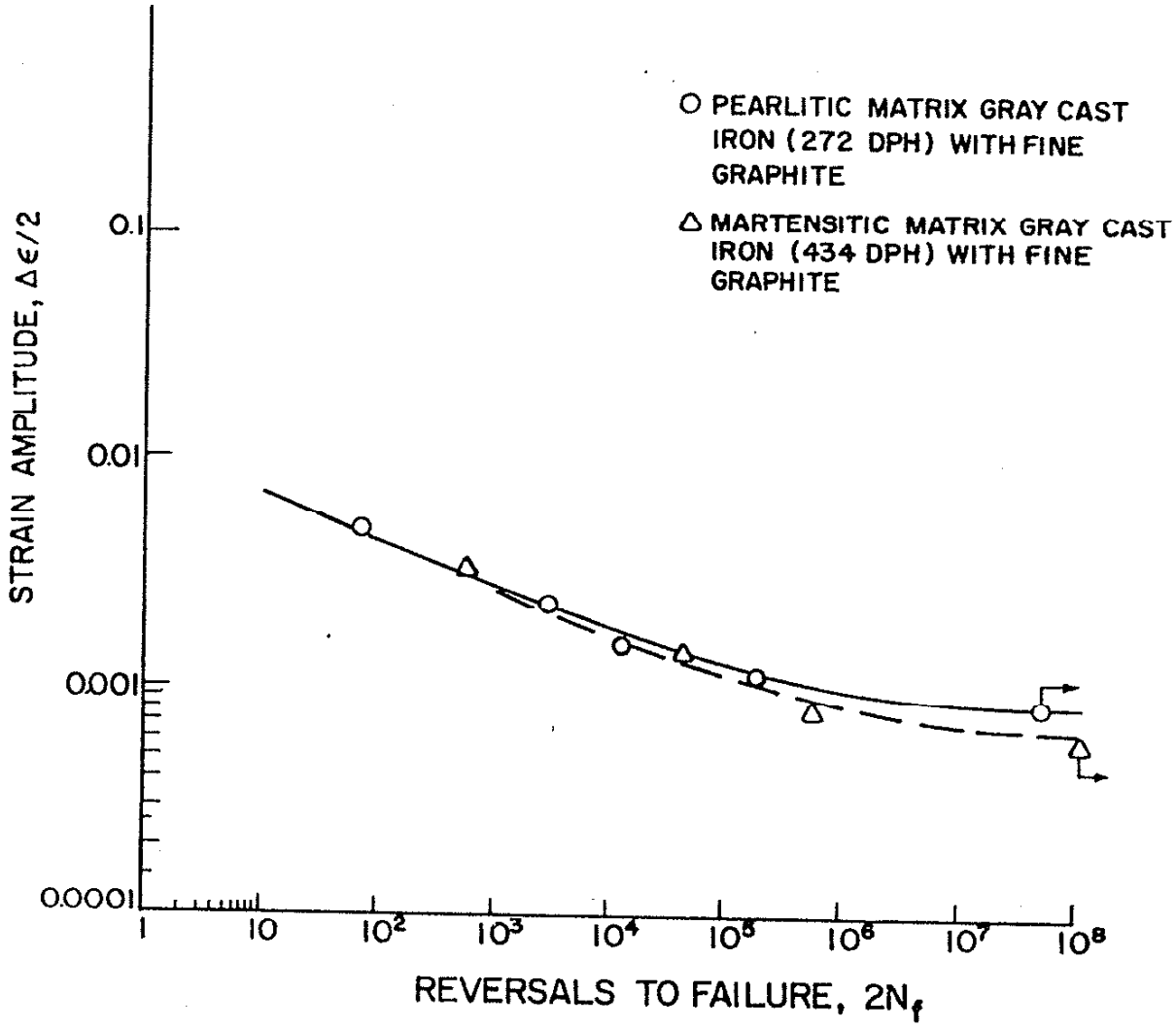

FIG. 20 STRAIN-LIFE CURVES FOR PEARLITIC (272 DPH) AND MARTENSITIC (434 DPH) GRAY CAST IRON WITH FINE GRAPHITE

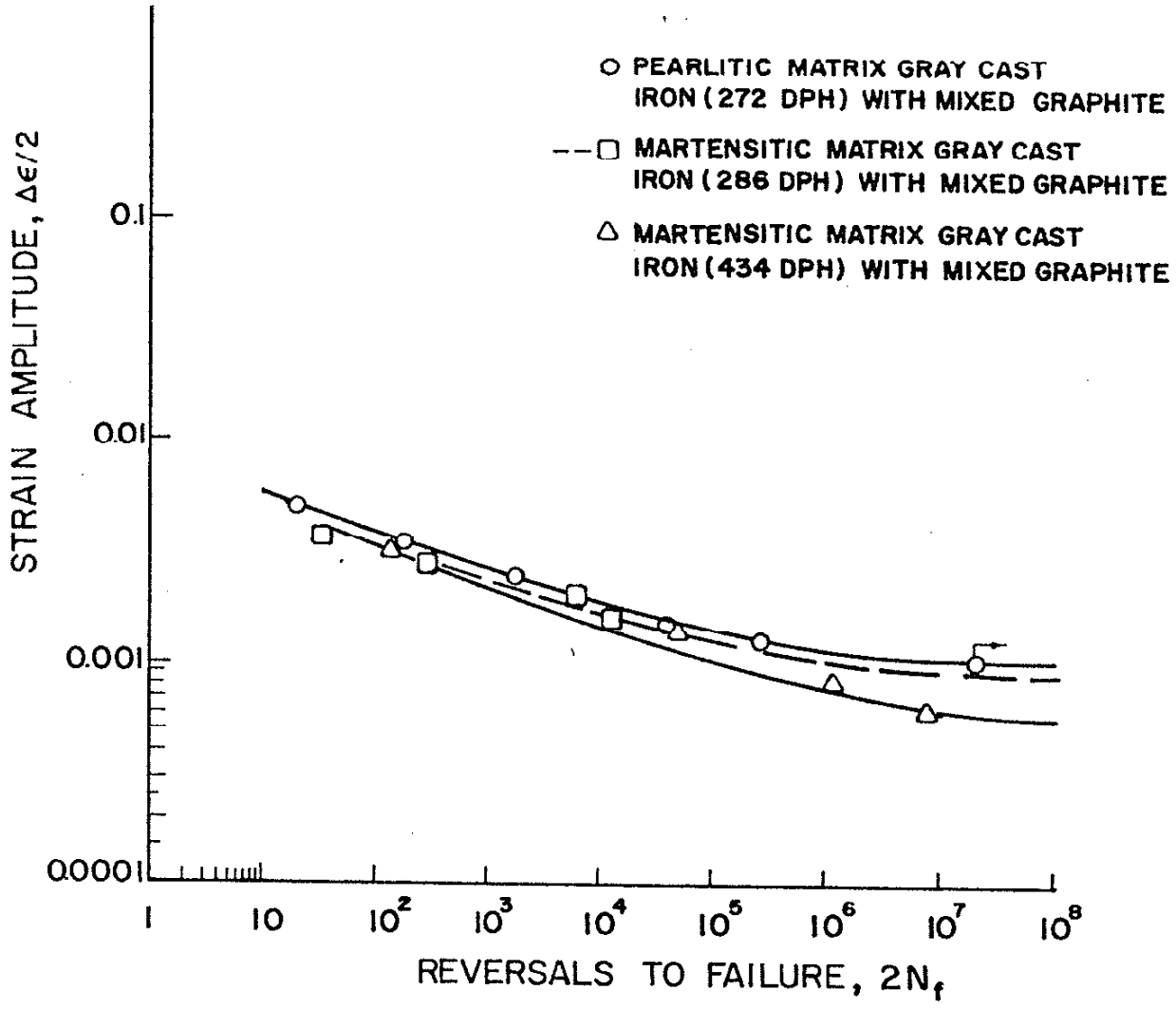

FIG. 21 STRAIN-LIFE CURVES FOR PEARLITIC (272 DPH) AND MARTENSITIC (286 AND 434 DPH) GRAY CAST IRON WITH MIXED GRAPHITE

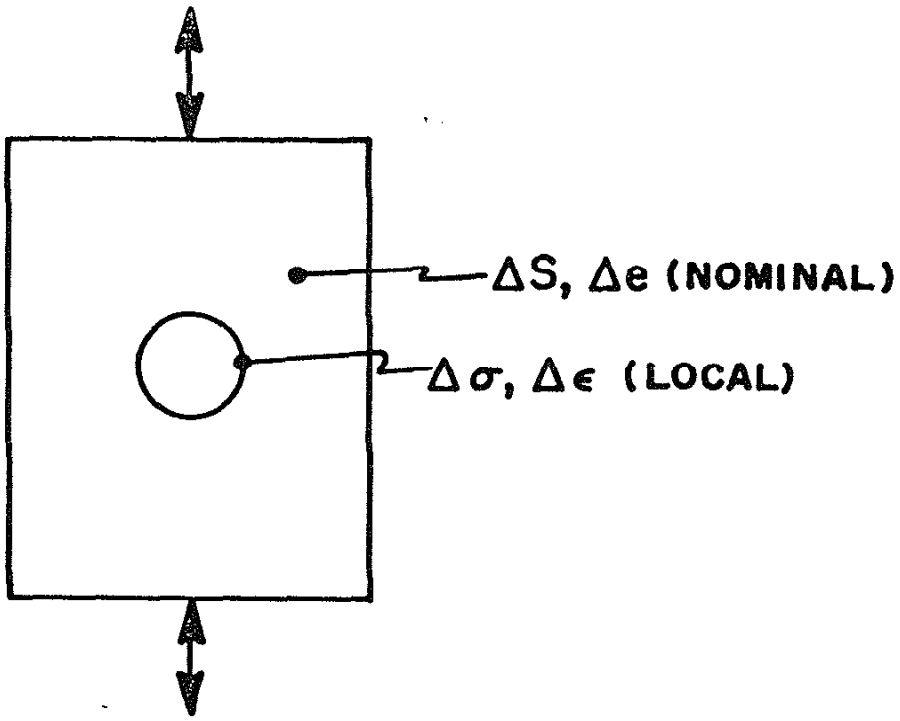

$$K_f(\Delta S \Delta e E)^{1/2} = (\Delta\sigma \Delta\epsilon E)^{1/2}$$

FIG. 22 REPRESENTATION OF PARAMETERS USED IN NEUBER ANALYSIS

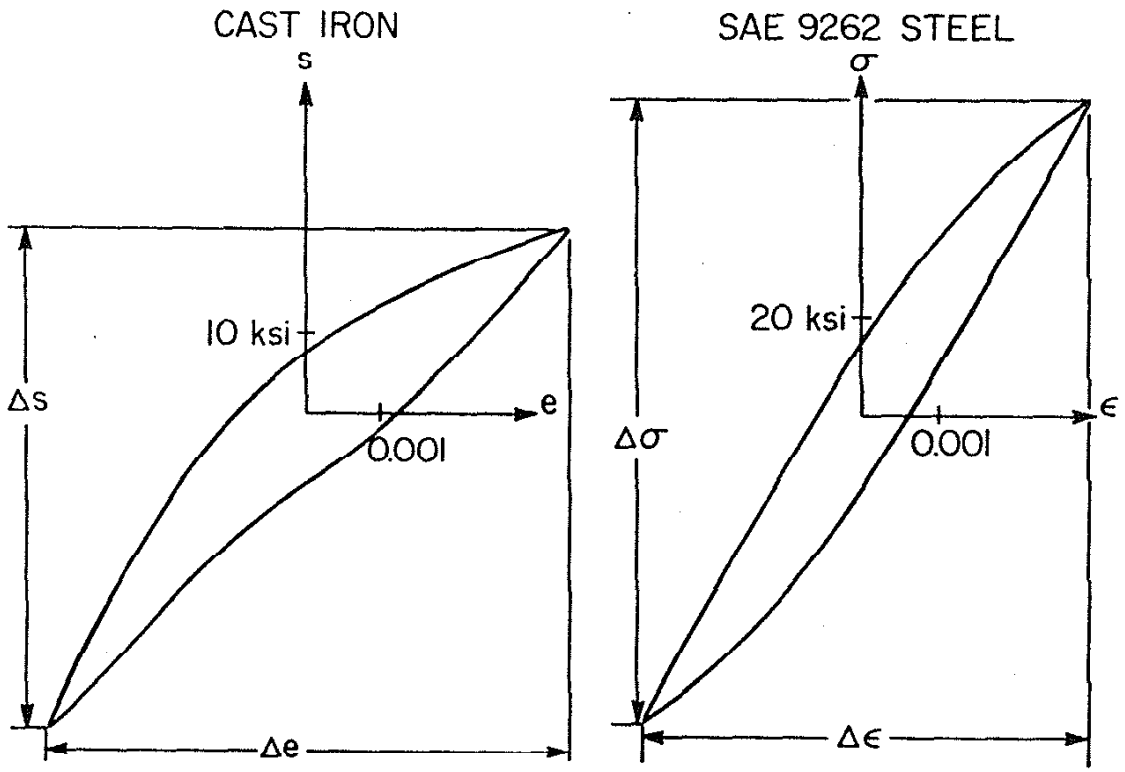

FIG. 23 REPRESENTATION OF PARAMETERS USED IN NEUBER ANALYSIS AS APPLIED TO GRAY CAST IRON AND STEEL OF EQUIVALENT STRUCTURE, HARDNESS AND COMPOSITION

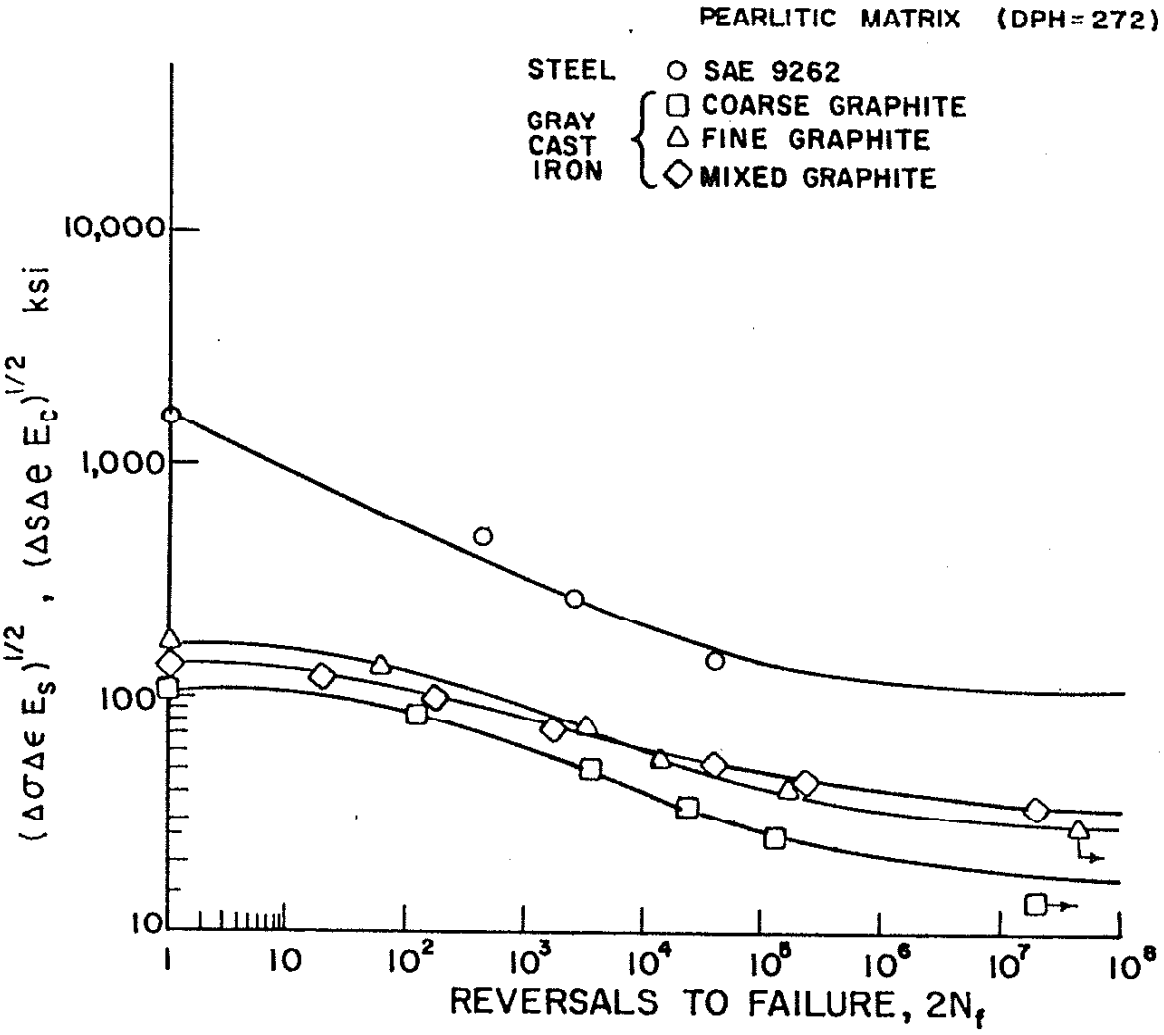

FIG. 24 NEUBER PARAMETER VS. REVERSALS TO FAILURE FOR STEEL AND GRAY CAST IRONS WITH PEARLITIC MATRIX (DPH = 272)

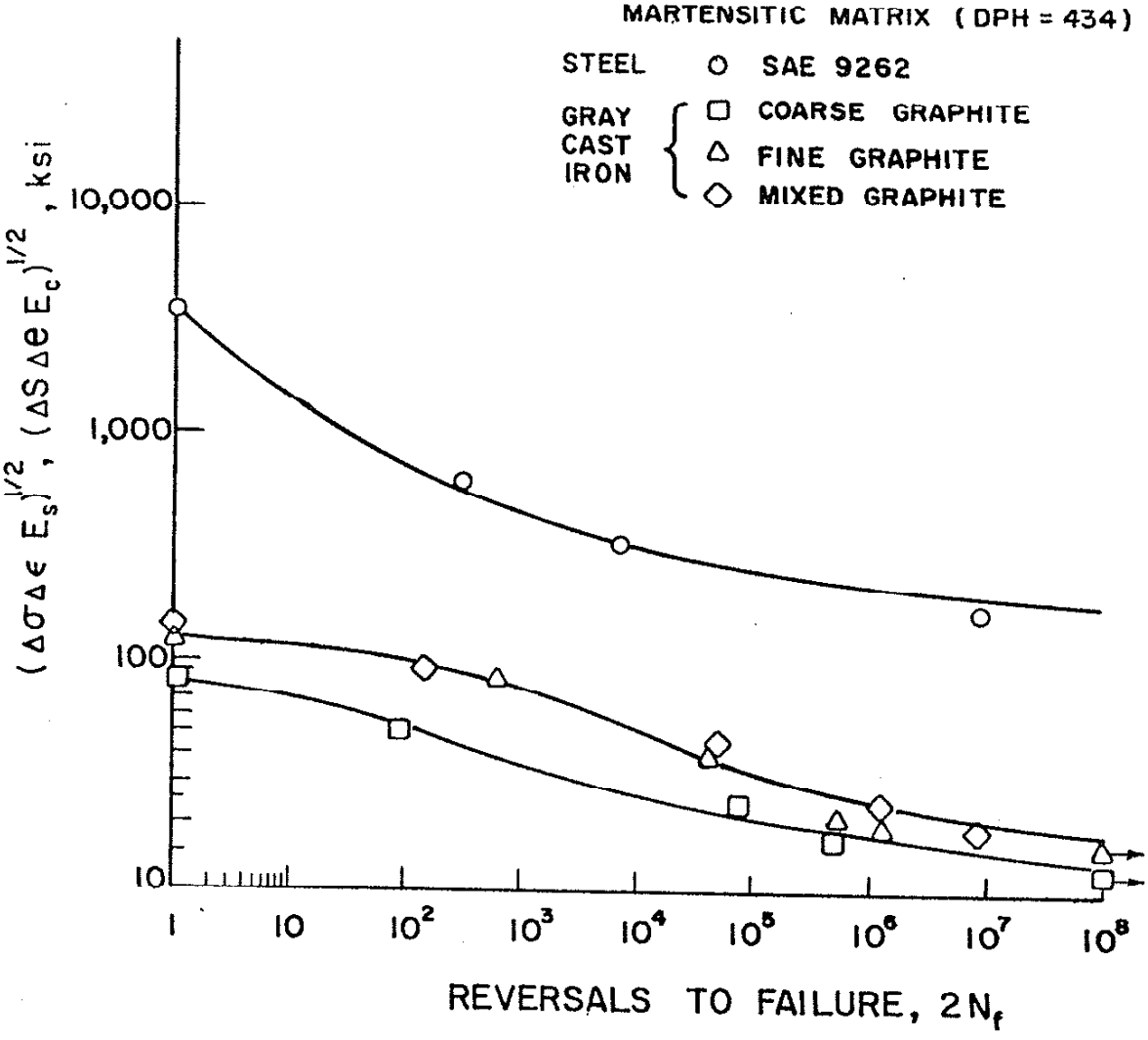

FIG. 25 NEUBER PARAMETER VS. REVERSALS TO FAILURE FOR STEEL AND GRAY CAST IRONS WITH MARTENSITIC MATRIX (DPH = 434)

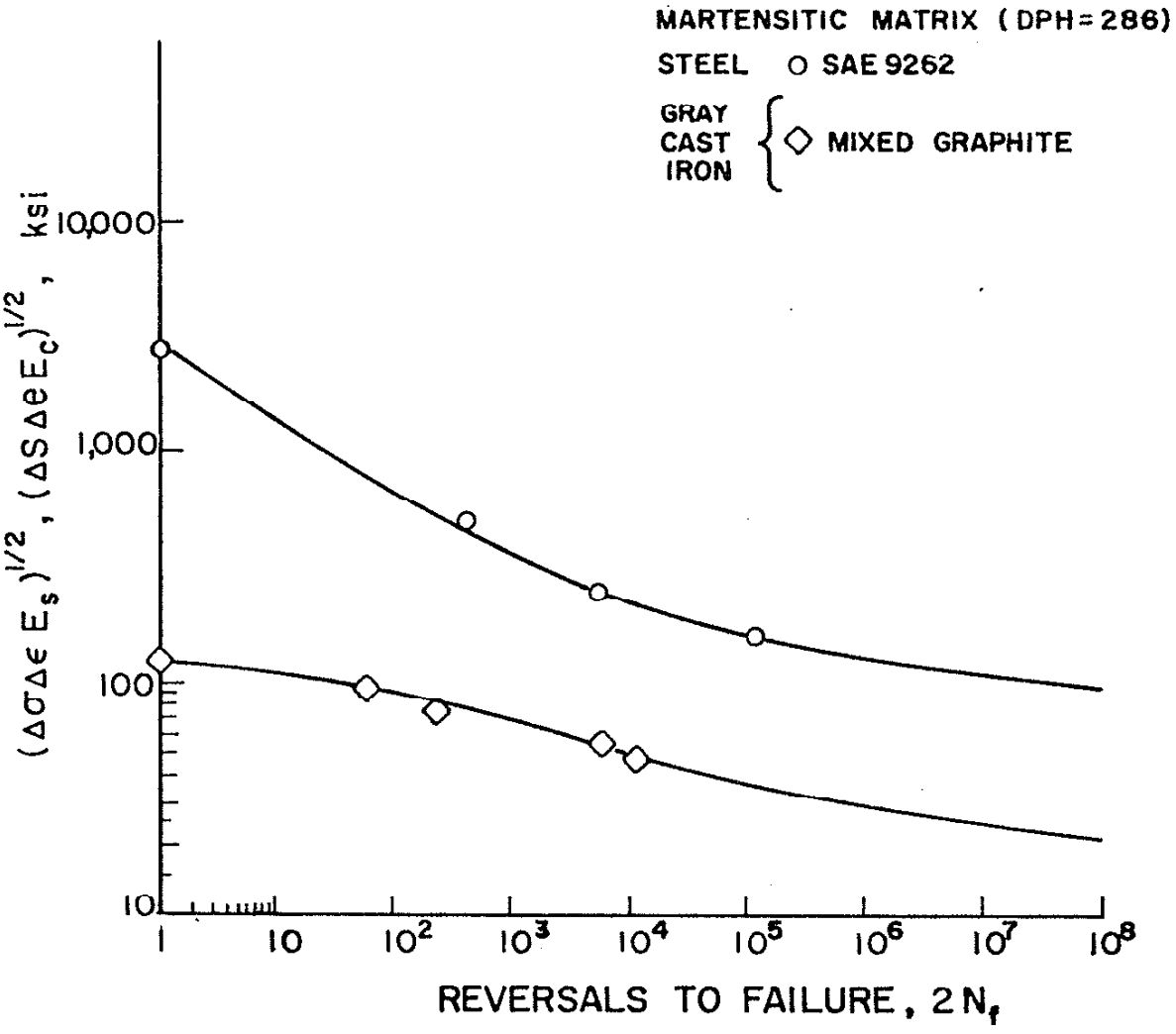

FIG. 26 NEUBER PARAMETER VS. REVERSALS TO FAILURE FOR STEEL AND GRAY CAST IRON WITH MARTENSITIC MATRIX (DPH = 286)

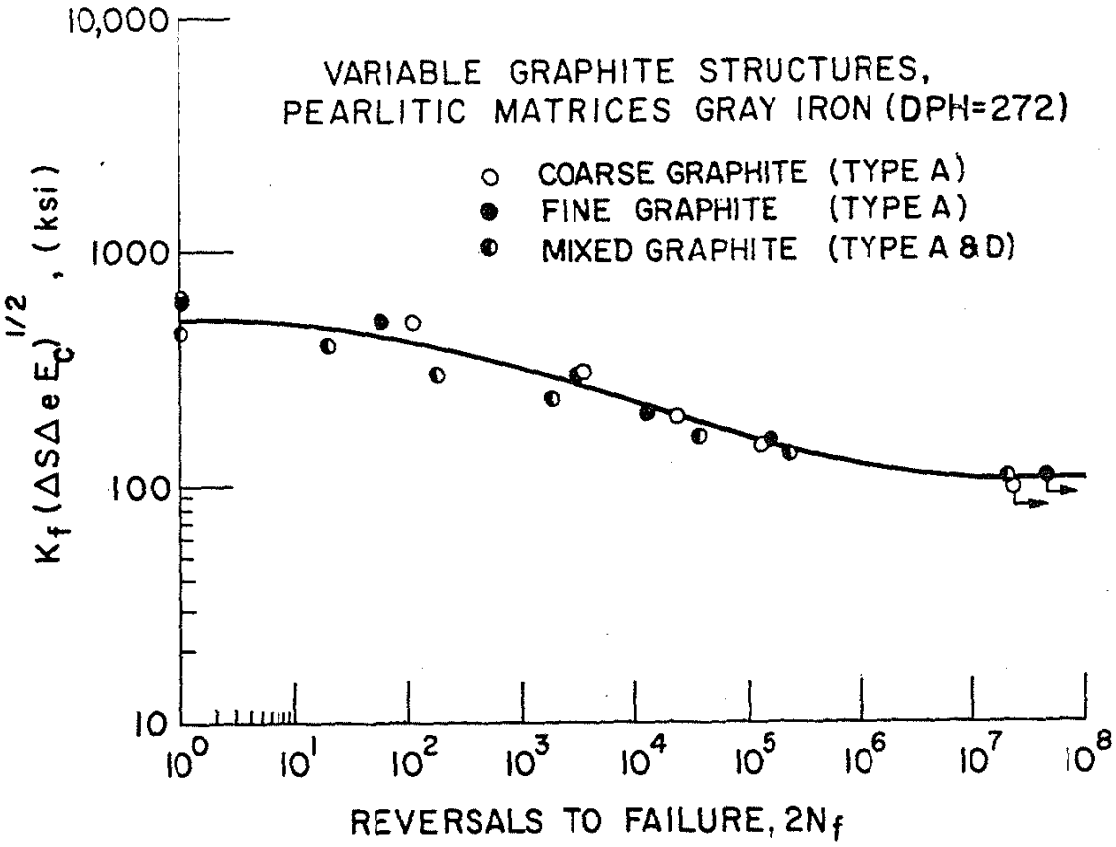

FIG. 27 MASTER PLOT OF NEUBER PARAMETER VS. REVERSALS TO FAILURE FOR PEARLITIC GRAY CAST IRONS WITH VARIABLE GRAPHITE STRUCTURES

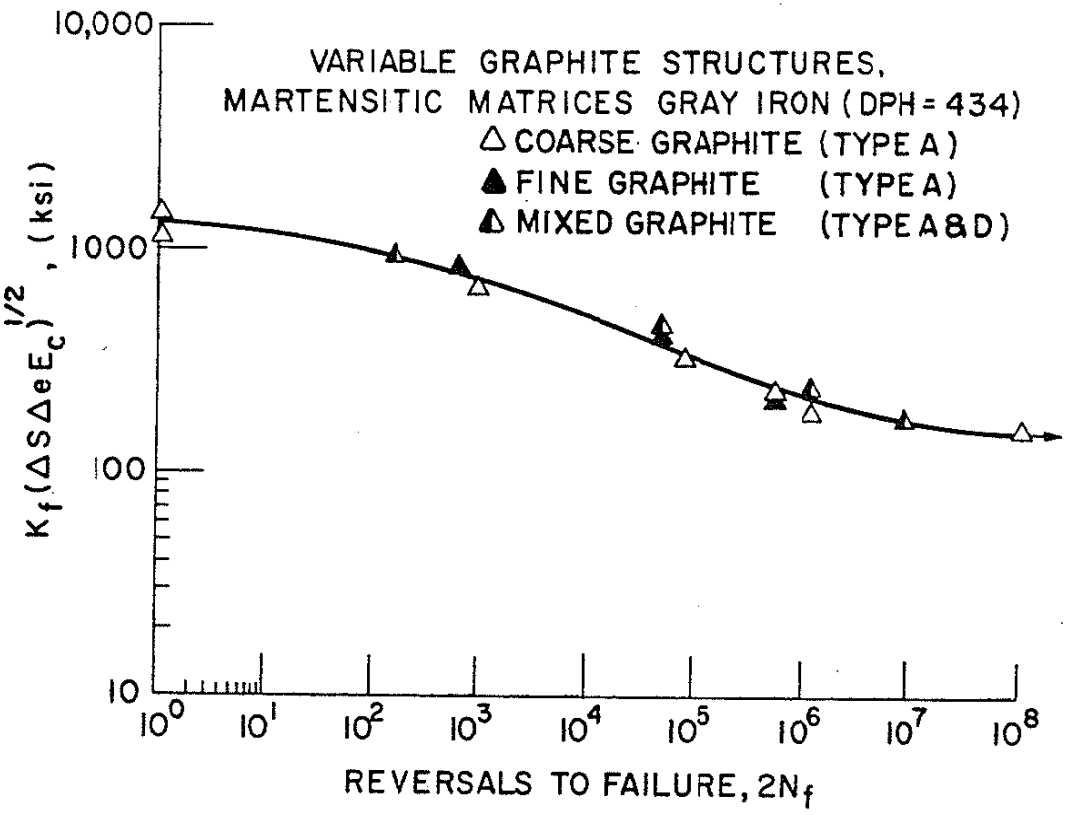

FIG. 28 MASTER PLOT OF NEUBER PARAMETER VS. REVERSALS TO FAILURE FOR MARTENSITIC GRAY CAST IRONS WITH VARIABLE GRAPHITE STRUCTURES

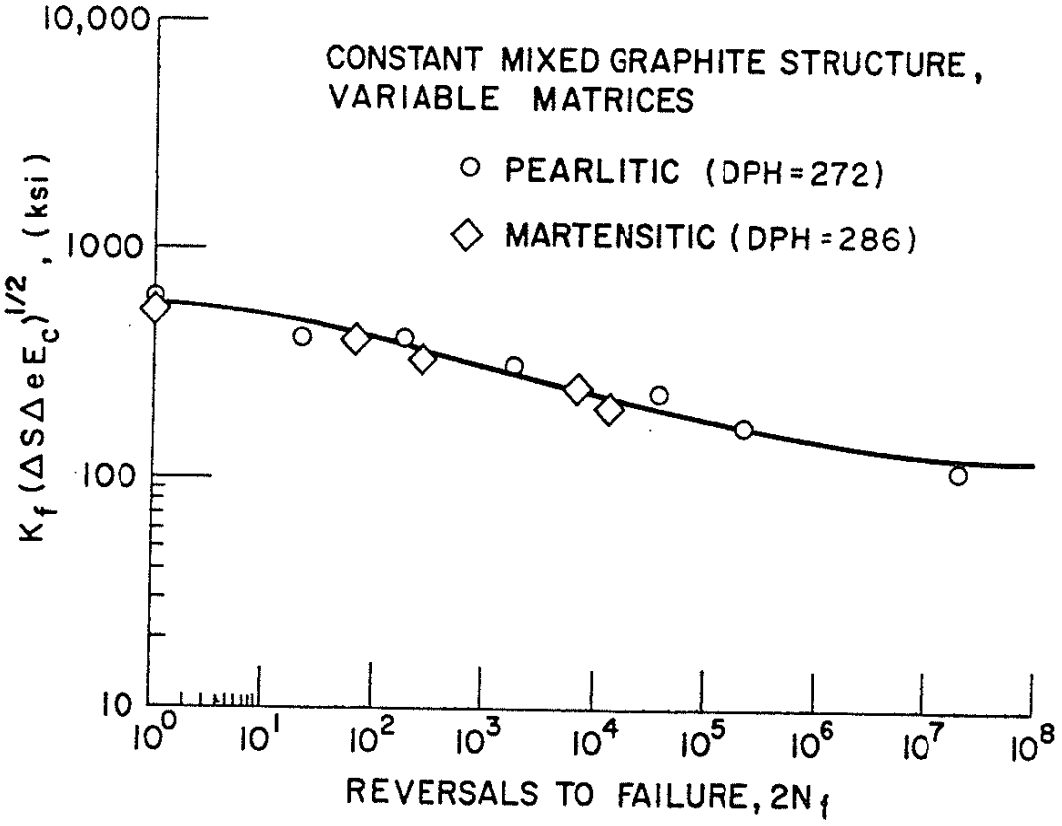

FIG. 29 MASTER PLOT OF NEUBER PARAMETER VS. REVERSALS TO FAILURE FOR MIXED GRAPHITE CAST IRONS WITH VARIABLE MATRIX STRUCTURES

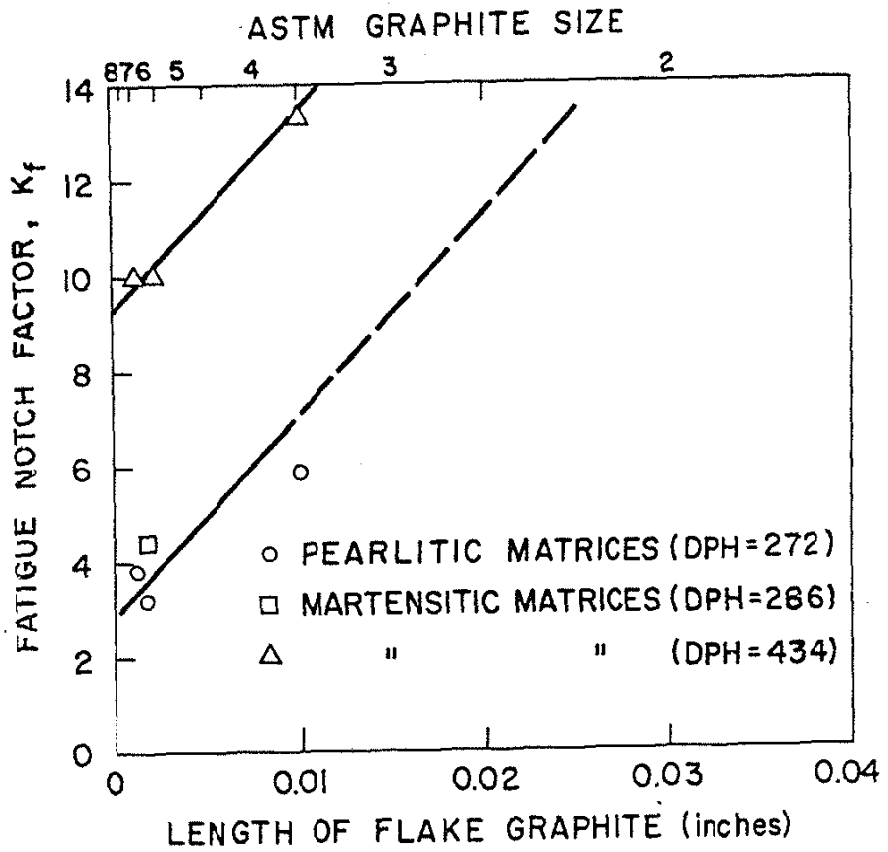

FIG. 30 FATIGUE NOTCH FACTOR VS. GRAPHITE FLAKE SIZE AT VARIOUS MATRIX HARDNESSES FOR GRAY CAST IRON

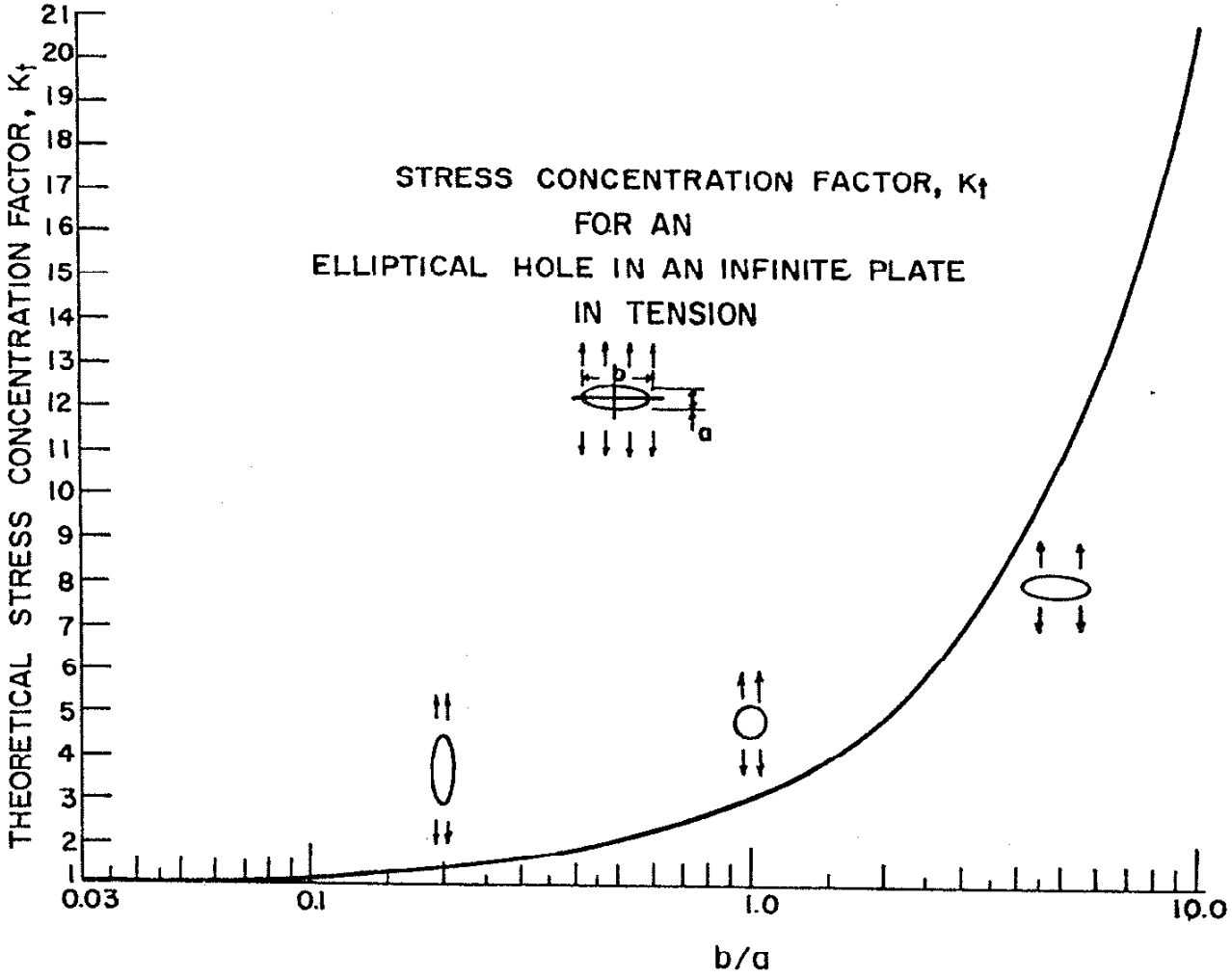

FIG. 31 THEORETICAL STRESS CONCENTRATION FACTOR (K_t) VS. ELLIPTICITY OF A HOLE IN AN INFINITE PLATE IN TENSION (PETERSON[12])

APPENDIX A

Heat-Treatments for SAE 9262 Steel and Gray Cast Irons

SAE 9262

Pearlitic Matrix (DPH = 272):

Austenitized for 1 hr at 1600°F

Isothermally transformed for 1 hr at 1300°F

Air cooled

Martensitic Matrix (DPH = 286):

Austenitized for 1 hr at 1600°F

Oil quenched

Tempered for 50 min at 1250°F

Martensitic Matrix (DPH = 434):

Austenitized for 1 hr at 1600°F

Oil quenched

Tempered for 1 hr at 900°F

Gray Cast Irons

Pearlitic Matrix (DPH = 272):*

As-cast condition. No heat-treatment performed

Martensitic Matrix (DPH = 286):*

Austenitized for 2 hrs at 1600°F then for 20 hrs at 1500°F

Agitated water quench

Tempered for 1 hr at 1200°F

Martensitic Matrix (DPH = 434):*

Austenitized for 2 hrs at 1600°F then for 20 hrs at 1500°F

Agitated water quench

Tempered for 25 mins at 400°F

---

*Matrix hardness measurement